RIDGE-TOP SPREADING FEATURES AND RELATIONSHIP TO EARTHQUAKES, SAN GABRIEL MOUNTAINS REGION, SOUTHERN CALIFORNIA -- PART B: PALEOSEISMIC INVESTIGATIONS OF RIDGE-TOP DEPRESSIONS

by
James P. McCalpin and Earl W. Hart
2002
Previously released as the following report:

RIDGETOP SPLITTING, SPREADING, AND SHATTERING RELATED TO EARTHQUAKES IN SOUTHERN CALIFORNIA

Final Technical Report
Contract 99HQGR0042
National Earthquake Hazards Reduction Program
U.S. Geological Survey

Principal Investigator:
James P. McCalpin
GEO-HAZ Consulting, Inc.
P.O. Box 837, 600 East Galena Ave.
Crestone, CO 81131
OFFICE: 719-256-5227
FAX: 719-256-5228
www.geohaz.com/geohaz

Co-PI
Earl W. Hart
6 Vista Court
Corte Madera, CA 94925

April 6, 2000

NON-TECHNICAL SUMMARY

The San Gabriel and eastern Santa Susana Mountains contain anomalous ridgetop depressions that resemble depressions formed or reactivated during large earthquakes elsewhere in California and worldwide. These depressions (sackungen) may constitute a ground-rupture hazard to buildings and utilities during earthquake shaking, so our maps show planners and engineers what ridgetop areas to avoid. The depressions may also preserve a record of prehistoric earthquake shaking in the form of displaced or deformed sediments. If true, these landforms could provide paleoearthquake histories.

In October 1999 we excavated 3 trenches across ridge-top depressions (sackungen) and mapped the fault structures and deformed deposits. All three trenches contained a record of 2-4 discrete prehistoric displacement events that had created their respective depressions. We were able to date buried soils and small pieces of charcoal in all three trenches, but not every displacement event could be bracketed tightly by radiocarbon dates. The latest event in the Blue Ridge and Lytle Creek trenches, which lay on ridgecrests adjacent to the San Andreas fault, could only be constrained to have occurred in a relatively broad time span. This time span overlapped the time spans of three prehistoric earthquakes dated by others in paleoseismic trenches on the San Andreas fault, so a one-to-one correlation could not be made between the sackung displacement event and a previously-dated earthquake.

The latest displacement at the Kagel Mountain sackung site just barely overlaps with the time range of the latest large prehistoric earthquake dated on the San Gabriel fault, which lies only 1 km from the sackung.

The main lessons we learned from this trenching investigation are: 1) sackung troughs do contain a record of prehistoric discrete displacement events that can be dated, and 2) to make a one-to-one correlation of these events to paleoearthquakes dated elsewhere, many more radiocarbon dates will have to be obtained from a single trench than we were able to afford under this grant.

TABLE OF CONTENTS

1. ABSTRACT....5
2. INTRODUCTION....6
    2.1 Acknowledgements....6
3. BLUE RIDGE TRENCH....8
    3.1 Location and Local geology....8
    3.2 Geomorphology....8
    3.3 Structure....11
    3.4 Stratigraphy....14
    3.5 Geochronology....17
    3.6 Interpretation....19
4. UPPER LYTLE CREEK RIDGE TRENCH....22
    4.1 Location and Local geology....22
    4.2 Geomorphology....22
    4.3 Structure....26
    4.4 Stratigraphy....28
    4.5 Geochronology....30
    4.6 Interpretation....31
5. KAGEL MOUNTAIN TRENCH....33
    5.1 Location and Local geology....33
    5.2 Geomorphology....34
    5.3 Structure....37
    5.4 Stratigraphy....40
    5.5 Geochronology....42
    5.6 Interpretation....43
6. DISCUSSION--ORIGIN OF RIDGETOP SPREADING IN SOUTHERN CALIFORNIA....45
7. CONCLUSIONS....47
8. RECOMMENDATIONS....48
9. REFERENCES....48

List of Figures **Page**

Fig. 1. Small-scale location maps of study area, showing all 3 trench sites 7
Fig. 2. Location map of the Blue Ridge trench site 9
Fig. 3. Topographic profile of Blue Ridge 10
Fig. 4. Topographic profile of the Blue Ridge trench site 10
Fig. 5. Log of the Blue Ridge trench 12
Fig. 6. Photograph of the south end of the Blue Ridge trench 13
Fig. 7. Inferred sequence of events that formed the Blue Ridge sackung 21
Fig. 8. Location map of the Upper Lytle Creek Ridge trench site 23
Fig. 9. Topographic profile of Upper Lytle Creek Ridge 24
Fig. 10. Photograph of the Upper Lytle Creek Ridge trench 25
Fig. 11. Topographic profile of the Upper Lytle Creek Ridge trench site 24
Fig. 12. Log of the Upper Lytle Creek Ridge trench 27
Fig. 13. Inferred sequence of events that formed the Upper Lytle Creek Ridge sackung 32
Fig. 14. Location map of the Kagel Mountain trench site 35
Fig. 15. Topographic profile of the Kagel Mountain ridge 36
Fig. 16. Detailed topographic map of the Kagel Mountain trench site 36
Fig. 17. Log of the Kagel Mountain trench 38
Fig. 18. Photograph of the main normal fault zone in the Kagel Mountain trench 39
Fig. 19. Schematic diagram of joint and foliation directions in the Kagel Mountain trench 41
Fig. 20. Inferred sequence of events that formed the Kagel Mountain sackung 44
Fig. 21. Space-time diagram showing ages of displacement events in our sackung trenches, versus ages of dated paleoearthquakes on nearby major active faults. 46

List of Tables

Table 1. Radiocarbon samples collected and dated in this study 18
Table 2. Comparison of paleoearthquake dates from the San Andreas fault to C-14 dates from the Blue Ridge trench 20

1. ABSTRACT

The San Gabriel and eastern Santa Susana Mountains contain anomalous ridgetop depressions that resemble depressions formed or reactivated during large earthquakes elsewhere in California and worldwide. We trenched three ridgetop troughs, two near the San Andreas fault in Pelona Schist, and one northeast of the San Fernando Valley in granitic gneiss.

Two of the three trenched ridgecrest troughs were the surface expressions of half-grabens with moderately dipping (45^{o}-65^{o}) normal faults*, whereas the third trough was underlain by a more symmetrical graben. The higher and steeper scarp on the surface did not necessarily overlie the master fault. In fact, at all three sites the higher surface scarp was developed on the hinged side of the graben, whereas the scarp atop the master fault was smaller but steeper. The 1-3 m of unconsolidated Holocene (?) slopewash beneath each trough was relatively coarse-grained (sand and gravelly sand) and poorly stratified. Accordingly, the main contacts mapped in these deposits were soil horizon boundaries. In places it was difficult to distinguish whether changes in color and texture were parent material contacts or soil horizon contacts.

The lower boundary of slopewash was gradational with weathered bedrock. The bedrock beneath the troughs was either extensively shattered (which we defined as "exploded bedrock") or chemically weathered from infiltration of water beneath the closed depression, much more so than beneath the flanking scarps.

Each trench exhibited stratigraphic evidence for 2-4 displacement events, but not all events could be tightly dated. In the Blue Ridge and Upper Lytle Creek Ridge trenches, the latest deformation event occurred after 790-867 cal yr. BP but before 285-300 cal yr. BP. This time span overlaps the age ranges of three dated paleoearthquakes on the San Andreas fault at the Wrightwood paleoseismic site of Fumal et al. (1993), only a few km west of the Blue Ridge trench. Thus, the dating constraints from the sackung trenches, due to the dispersed nature of soil organics and charcoal, are not tight enough to make a positive correlation with any particular paleoearthquake on the San Andreas fault. The older displacement events at Blue Ridge and Upper Lytle Creek Ridge are generally older than the oldest dated event in the Wrightwood or Pallet Creek chronologies.

The latest displacement event at the Kagel Mountain site is relatively well bracketed between 1830 and 2355 cal yr. BP. This age range barely overlaps with the age range of the latest paleoearthquake on the San Gabriel fault, the closest active fault to the site, as dated by Cotton et al between 907 and 1993 cal. yr BP.

We have demonstrated that sackung troughs contain a stratigraphic record of repeated displacement events that can be dated. However, given the type and distribution of carbon in the trough deposits, it will require 2-3 times as many radiocarbon dates as we had budgeted for to bracket event dates well enough to compare them with paleoearthquake chronologies from trench studies.

*As used here, the term fault describes a well-defined fracture that has measurable displacement but is a surficial feature that dies out at depth.

2. INTRODUCTION

During May 1998 we mapped ridgetop troughs and scarps on the mountains north of the Los Angeles Basin, to identify landforms and sediment traps likely formed by strong earthquake shaking and subsequent ridge collapse (sackungen). The results of this mapping are contained in our Final Technical Report for FY 1998 for NEHRP contract 98-HQ-GR-1026 (McCalpin and Hart, 1999). In 1999 we excavated three trenches across linear troughs on ridgetops in the eastern and western San Gabriel Mountains (Figure 2).

During October 1999 we spent 2.5 weeks excavating, logging, and sampling three trenches across ridgetop collapse landforms. The sites were: 1) summit of Blue Ridge directly south of Wrightwood, 2) summit of Upper Lytle Creek Ridge directly south of the Sharpless Ranch, and 3) summit of the ridge about 1 km east of Kagel Mountain, southeast of Pacoima Reservoir (Fig. 1).

The goal of this trenching investigation was to describe, for the first time in southern California, the structure and stratigraphy beneath these troughs and scarps, and to see if they indicated whether the troughs were formed by slow creep (Zischinsky, 1966, 1969; Tabor, 1971; Radbruch-Hall et al., 1976, 1977; Radbruch-Hall, 1978; Varnes et al., 1989) or by sudden vertical displacements, as observed after several California earthquakes elsewhere (Hart et al., 1990; McCrink, 1995; Nolan and Weber, 1992; Ponti and Wells, 1991; Spittler and Harp, 1990; Technical Advisory Group, 1991; Harp and Jibson, 1996) . If the latter, we wished to apply standard paleoseismic techniques developed for active normal faults to determine the amount and timing of the displacement event(s). The timing of these events, as dated by radiocarbon, would then be compared to the known paleoseismic histories of area faults to see if they coincided. If they did coincide, we would conclude that these ridge-top "sackungen" were probably formed by ridge crest collapse during severe earthquake shaking. Such a conclusion would mean that sackung troughs could be added to the suite of secondary paleoseismic evidence (as defined by McCalpin and Nelson, 1996). Such an addition would have worldwide implications, particularly in areas where seismogenic faults do not create surface fault scarps, such as in active fold and thrust belts.

Conversely, if the dates of sackung displacement events fall between those of any known paleoseismic fault history, it implies either that: 1) severe shaking is not the cause of these troughs, or 2) the troughs were created by shaking from a fault that does not yet have a known paleoseismic history. In the Los Angeles Basin such a fault could be a blind thrust, such as the Hollywood fault (Dolan et al, 1997) or the causative fault of the 1994 Northridge earthquake. In that case, presumably future paleoseismic studies on the blind thrusts might some day date these same events, using techniques that have not yet been developed.

2.1 Acknowledgements

This study would not have been possible without the assistance of many people. Permission to trench on National Forest land was granted by Rangers Steve Carbaugh (Santa Clara/Mojave River Ranger District, Angeles National Forest) and Bruce Quintelier (Los Angeles River District, Angeles National Forest). Sharon Dougherty (Circle Mountain Biological Consultants, Wrightwood, CA) performed an outstanding biological/ botanical survey of the Kagel Mtn. and Blue Ridge sites, while Debby Hyde-Sato (San Bernadino National Forest) cleared the Lytle Creek Ridge site. Joe Simon (W and S Consultants, Simi Valley, CA) performed the cultural resources survey of the trench sites and shared with us his eyewitness observations of ridgetop spreading during the 1994 Northridge earthquake. We thank Gary Buzza (Buzza Backhoe, Agoura Hills, CA) for excavating the trenches, and

Jim Reed (Reed's Tractor, Phelan, CA) for backfilling them. Molly Zorba (Earth Consultants International, Orange, CA) assisted in logging the Kagel Mountain trench. Randy Jibson (USGS) and Jerry Treiman (CDMG) shared their knowledge of ridgetop spreading and landsliding. Finally, we thank the California Division of Mines & Geology for their support.

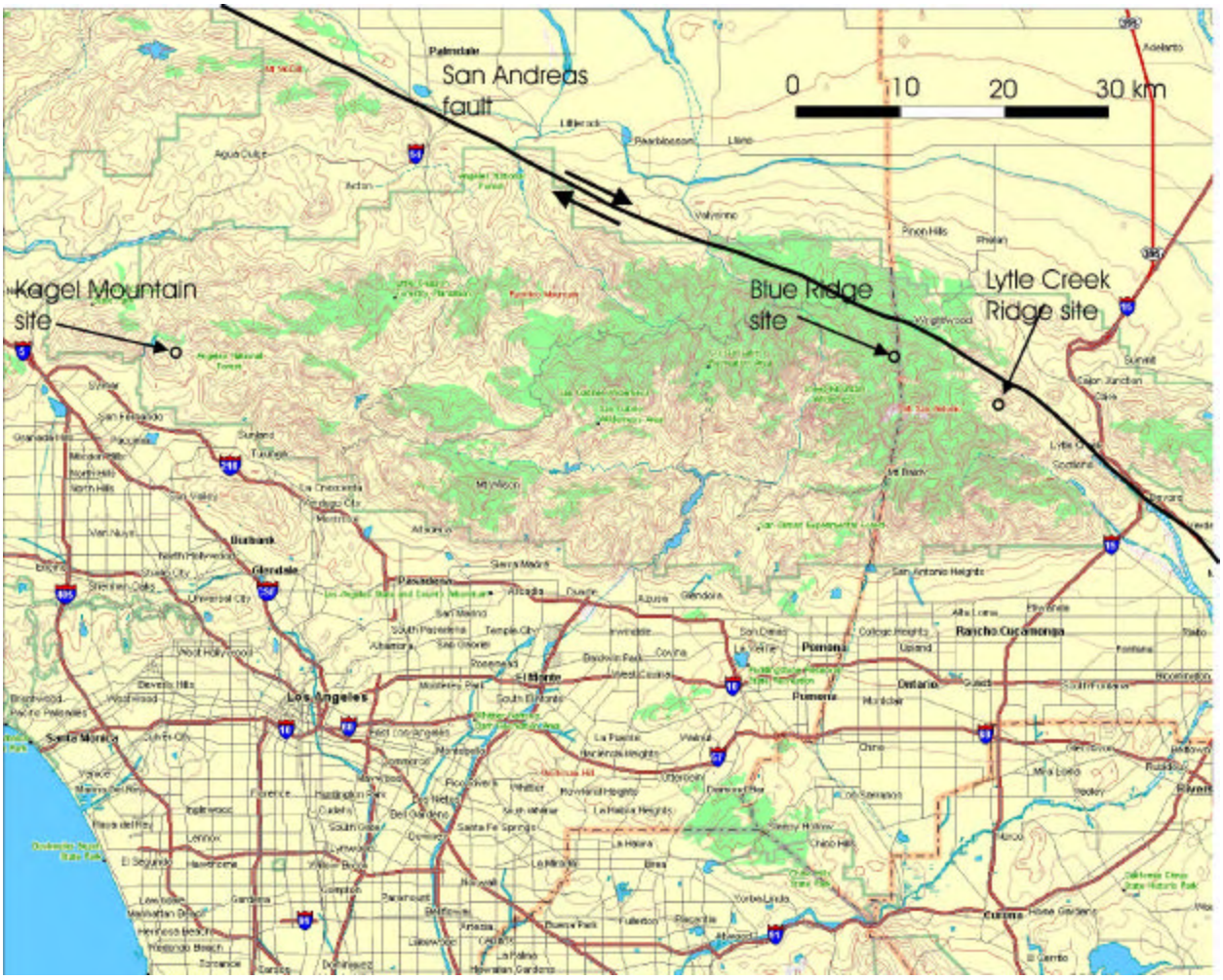

Fig. 1. Small-scale location map of study area, showing all 3 trench sites.

3. BLUE RIDGE TRENCH

3.1 Location and Local geology

The Blue Ridge trench was located on the summit of Blue Ridge at 8100 ft elevation, about 2 km south of the town of Wrightwood and the trace of the San Andreas fault (Fig. 2). This ridge descends to Swarthout Valley to north (Fig. 3) and to the higher-level valley of upper Prairie Fork to the south. The ridge crest contains numerous troughs and upslope-facing scarps, which are relatively scarce near the Angeles Crest Highway, but become more numerous toward Wright Mountain. Some of these scarps are described in a road log by Morton and Sadler (1989). To reach this site, turn west off the Angeles Crest Highway (California Highway 2) onto Forest Road 3N06, which travels east on the crest of Blue Ridge. The trench is located 5.8 miles east of Highway 2.

Blue Ridge trends generally east-west and is composed of Pelona Schist (Jennings and Strand, 1969), a fissile muscovite-albite-quartz schist that is "the most landslide-prone...basement rock type of inland southern California" (Morton and Sadler, 1989, p. 301). Very large, active landslides occur on the north slope of the ridge above the town of Wrightwood, and also on the north slope of Pine Mountain southeast of our trench site. Foliation at the trench site strikes N55^{o}E and dips 40^{o}E.

3.2 Geomorphology

The trench transected a 5 m-wide, 100 m-long ridgetop trough developed in Pelona Schist. Morton and Sadler (1989, p. 319) pointed out this feature and termed it "a very pronounced ridge-top trench. Look for marker posts in the trench. [Note: our backhoe trench exhumed one of these old wooden marker posts]. *We consider this trench to be part of a typical sackung that has developed on a high-relief ridge* [italics added] in contrast to the spreads and trenches on the low ridges in Lone Pine Canyon" (discussed in Sec. 4).

We trenched the trough about 10 m east of the boundary line between Los Angeles and San Bernardino Counties. The Pacific Crest Trail runs east-west directly south of the trough, and our trench stopped just short of transecting the Trail. The trough at the trench site is asymmetrical, with a lower (0.8 m-high) but steeper scarp on the south side and a slightly higher but gentler scarp on the north side (Fig. 4). The maximum scarp slope angle on the 0.8 m-high scarp was 35 degrees, suggesting relatively recent displacement.

The ridge crest on which this sackung occurs is asymmetrical, with a steep (37^{o}) slope descending north toward Wrightwood, and a gentler southern slope. The northern slope is near or at the angle of repose, and landslide scars exist farther downslope. However, based on a rather cursory examination there is no landslide toe visible that might be connected to the ridge-crest trough. In other words, it does not appear that the trough is simply the head of a landslide. The south slope of the ridge is gentler, having a far-field slope angle of about 24^{o}.

About 5 m west of our trench the southern scarp that we trenched dies out and the displacement transfers to a parallel strand about 2 m farther south. This left stepover zone lies just west of our trench and may indicate a component of right-lateral slip in the sackung zone. The southern scarp slowly dies out as traced toward our trench, and its only indication in our trench is the shallow sag pond partially exposed at the south end of our trench, and two underlying fracture zones, one of which contains open voids.

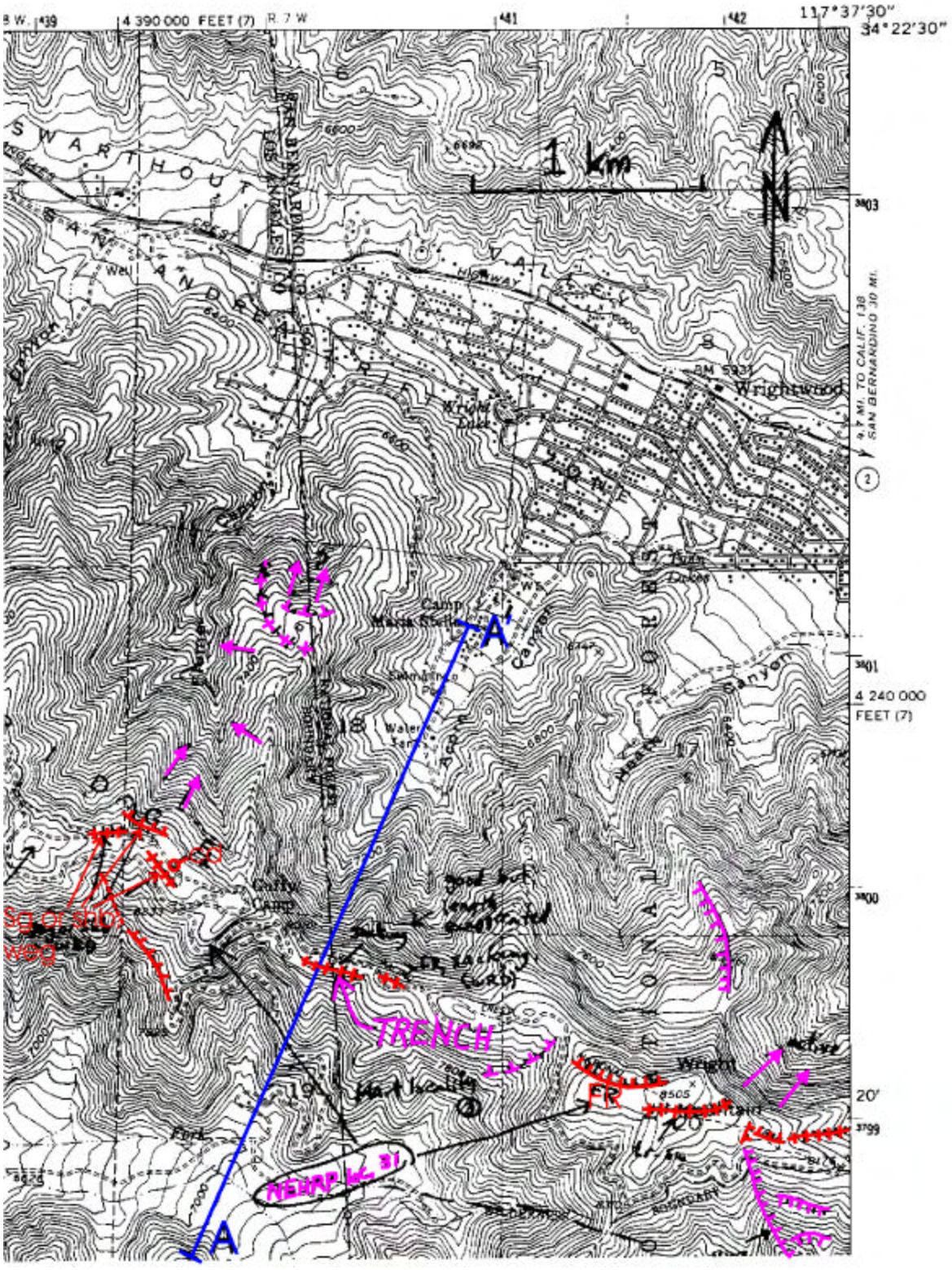

Fig. 2. Location map of the Blue Ridge trench site, from McCalpin & Hart, 1999 (Mt. San Antonio 7.5' quadrangle). Symbols: trough (tr/ railroad tracks); scarp (line with tick marks); closed depression (cd); flattened ridge (FR); landslide (ls/ barbed arrows, dashed line for boundaries); bench (b); sidehill bench (shb); back-facing scarp (bfs); swale (sw).

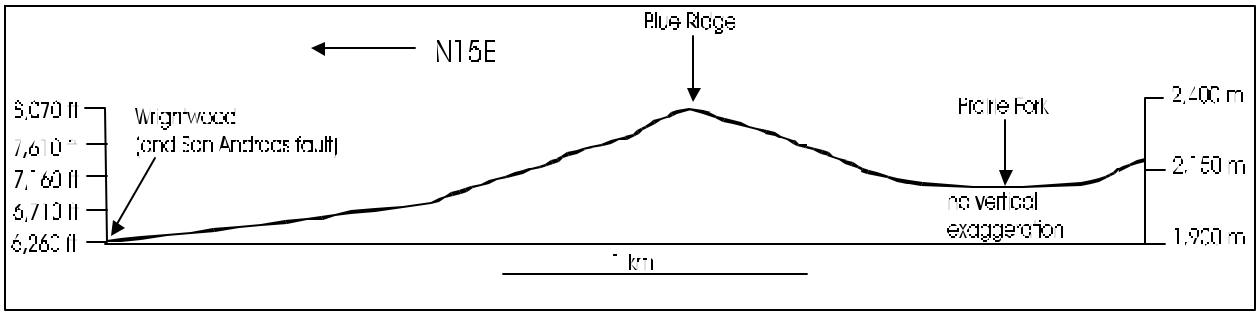

Fig. 3. Topographic profile of Blue Ridge.

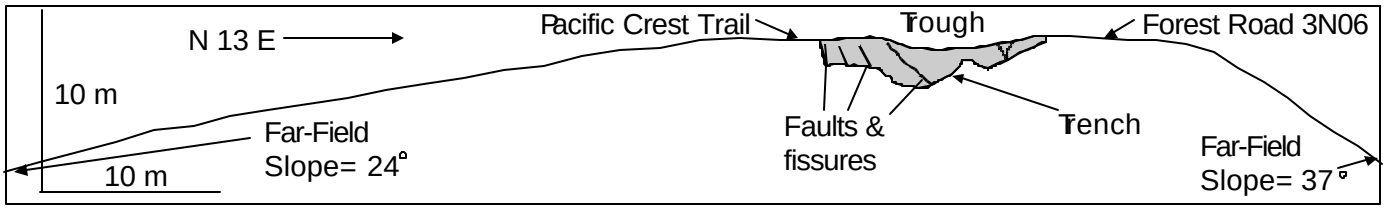

Fig. 4. Topographic profile of the Blue Ridge trench site.

3.3 Structure

The topographic trough is the surface expression of a south tilted half-graben, with a main normal fault zone (composed of faults F5 and F6) beneath the southern scarp (Fig. 5). The two faults comprising this zone differ significantly in structure. Fault F6 juxtaposes schist bedrock against schist bedrock, and is defined by a 10 cm-thick zone of broken schist in which tabular schist rubble has been reoriented with long axes parallel to the fault zone. This shear zone dips about 45^{o} north. It is not clear how much net slip has occurred on fault F6, because the only stratigraphic marker in bedrock of the footwall (clay gouge) is not exposed on the hanging wall. Its absence argues for a net slip of at least 1.5 m. A large tension fissure (filled with crack fill unit cf4) splays off the middle of F6.

Although F6 clearly has experienced normal slip, it could not be traced above the top of bedrock as a continuous feature to the ground surface. Instead, the main normal fault that approaches the ground surface (fault F5) is steeper (50-60^{o} north dip), lacks obvious shear fabric, is a single thin fault plane, has no associated tension fissures, and steepens to a near-vertical dip once it intersects the top of bedrock. Altogether this fault displays less evidence of extensional dilation along the fault plane, and more resembles tectonic normal faults observed in trenches elsewhere in the western USA (e.g. McCalpin, 1996a).

Fault F5 only comes within 40 cm (horizontal) of the top of F6, but does not appear to connect with F6. However, that 40 cm space is occupied by alluvium (units al2b and al2a) that dips north and may have been dragged along the fault zone, thus faults F5 and F6 may be connected via a zone of diffuse shearing in this alluvium. The lowest, near-vertical part of F5 only offsets the top of the clay gouge unit by about 20-30 cm, and that displacement is not enough to have created the topographic trough. Thus, the >1.5 m of net slip on F6 must transfer to the upper, 50-60^{o} part of F5 in the vicinity of units al2a and al2b, but we could not see exactly how this occurred.

The bedrock between F5 and F6 near the floor of the trench is extensively fractured and many of the fractures are open 1-3 cm, as if dilated. This was the only section of the trench wall to cave in, as joint-bounded blocks fell out of the wall, creating an overhang on both walls of the trench.

The uppermost 30 cm of F5 appears to define a depositional free face contact with the youngest colluvium (unit c1AC). Older units (in descending order, units c2A, s2AC, al3b, al3a) are truncated by the fault. This geometry indicates that the surface trough was created by normal slip on F5, and that the trough has filled in with a combination of scarp-derived colluvium (e.g., units c1AC, c2A) and slopewash and alluvium deposited along the axis of the trough.

The footwall of main normal fault zone is cut by three normal faults with smaller displacements (from south to north, 0.2 m [F2], 0.4 m [F3], and 0.25 m [F4]). The parallelism of these faults and the south dip of the top of bedrock suggests these faults bound "domino" blocks of Pelona Schist that are being rotated counterclockwise (as viewed on the trench log) by north-south extension.

The south end exposes a tension fissure (F1) that does not offset the top of bedrock vertically. This tension fissure, which contains open voids (white areas on Fig. 5), underlies a shallow topographic depression at the surface that has been filled with clast-poor sag pond silts and sands. This depression defines the east end of a north-facing topographic scarp that becomes higher to the west until it becomes the main southern boundary scarp of the trough.

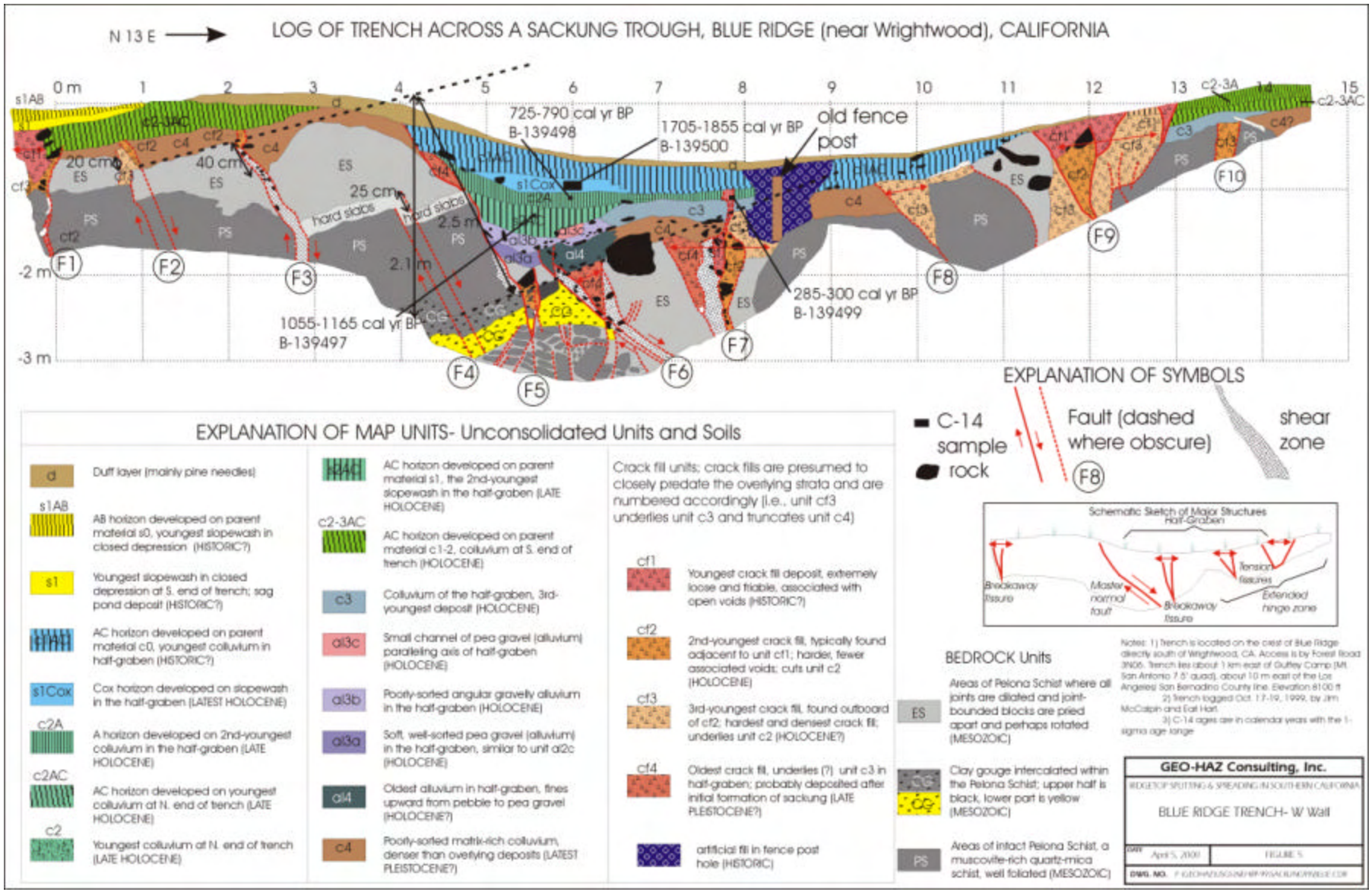

Fig. 5. Log of the Blue Ridge trench.

Fig. 6. Photograph of the master normal fault zone in the Blue Ridge trench. The red flags on the wall in front of J.P. McCalpin outline fault F6, the top of which is at the end of tape measure. Fault F5 is outlined by green flags. The very white rock to the left of the green flags is the Pelona Schist. The brown material between McCalpin and the trench shore (far right) is the sequence of unconsolidated deposits beneath the trough. Photograph by Earl Hart, Oct. 31, 1999. Yes, it was cold at 8100 ft elevation that day.

Fault F7 is actually a complex zone of filled tension fissures of three different ages. This extensional zone separates domains with two different backtilt angles, a southern zone beneath the trough axis tilted 20^{o} toward the main normal fault, and a northern zone beneath the northern boundary scarp tilted 10^{o} south. The greater rotation of the block beneath the trough has caused the upper part of it to pull away from the northern block.

Faults F8, F9, and F10 are also tensional fissures that underlie the northern boundary scarp. These fissures show vertical offsets of 30-50 cm on the top of bedrock, but the net throw across F8 and F9 is negligible. They probably result from the downward flexure of this limb of the half-graben toward the main normal fault (faults F5 and F6).

3.4 Stratigraphy

We distinguished 3 bedrock map units and 20 unconsolidated map units in this trench. Criteria for defining units and the techniques of logging follow those described by McCalpin (1996b).

3.4.1 Bedrock Map Units

We divided the Pelona Schist into 3 mapping units. Unit PS represents areas of relatively intact schist that exhibits a consistent foliation. Although some joints are dilated, the schist blocks have not been rotated out of position. The joints themselves do not contain a large amount of unconsolidated fill. Unit CG is a zone of clay within the Pelona Schist that contains few small angular shards of schist. It looks like clay gouge associated with faulting, but its orientation roughly perpendicular to the main normal fault zone indicates that if it is gouge, it was not created by movement on these sackung structures. Also, it is unlikely that such gouge could be formed within 2-3 m of the ground surface, where there is essentially no confining pressure. The structures associated with the sackung landform indicate dilation, north-south extension and brittle rupture, whereas forming a clay gouge would require considerable confining stress normal to the fault zone and quasi-plastic deformation. For these reasons we believe that this clay gouge represents an old fault zone in the Pelona Schist that is unrelated to the extensional development of the sackung, and predates the present topography. Roadcuts in the Pelona Schist elsewhere on Blue Ridge commonly exhibit such clayey "gouge" zones, but these have no surface expression.

A unique map unit used here is "exploded schist" (ES). This unit represents areas of Pelona Schist where schist blocks have rotated out of their original orientation and now display various foliation directions. The joints are partly to wholly filled with smaller schist rubble but this rubble does not contain any colluvial or slopewash material derived from Quaternary unconsolidated units; it is all crushed schist. These areas look like the rock was blasted with explosives ("exploded") and all the joints were opened enough that schist blocks could rotate.

3.4.2 Unconsolidated Units

The unconsolidated map units defined in this trench include both parent materials unaffected by soil formation (e.g., al3b), and parent materials that have been affected by soil formation (e.g., c1AC). In the latter group the map units were defined by changes in soil horizon properties, rather than by a change in parent material sedimentology. For example, at the south end of the trench the lower part of parent material s1 (youngest slopewash in the sag pond) is not affected by soil formation, so its map designation is simply s1. Its upper part has been incorporated into the AB horizon of the surface

soil, hence that part of the unit is mapped as s1AB, with the parent material abbreviation forming the fist part of the map unit designation and the soil horizon name forming the last part of the map unit designation. This same naming convention is used throughout the trench.

The unconsolidated deposits exposed in the trench form three local stratigraphic sequences deposited in three different structural domains. These domains are: 1) footwall of the main normal fault, 0-3 m on log horizontal scale; 2) hanging wall beneath the trough axis, between 4 and 11 m; and 3) hanging wall beneath the northern boundary scarp, between 13 and 15 m. The boundaries between these three sequences are bedrock highs, between 3-4 m and at 11 m on the horizontal scale of the log. Over each bedrock high the unconsolidated deposits have been thinned by erosion and many units disappear altogether, thus one must correlate between sequences. Below, we describe each stratigraphic sequence separately.

3.4.2.1 Deposits Beneath the Trough Axis

Unconsolidated deposits are thickest beneath the trough axis (1.5 m) and are divisible into the most units. The oldest deposits are crack (fissure) fills (unit cf4) that penetrate bedrock (exploded schist) and are overlain by the oldest stratiform deposits. These crack fill deposits are poorly-sorted, matrix-supported gravelly silty sands, with angular, tabular schist clasts. Their degree of hardness and density are similar to that of the layers directly above them.

The oldest stratiform deposit is a 30 cm-thick layer of weakly stratified, moderately-sorted alluvium (al4), which grades away from the fault into a matrix-rich, poorly sorted colluvium (c4). The alluvium grades from an angular, small pebble gravel upward to a subangular, pea gravel. The lens shape of the deposit suggests the alluvium is an elongate channel deposit that runs down the axis of the trough. These deposits are the densest and hardest in the trough sequence. At present they dip about 20^{o} south, toward the fault.

Overlying the units al4 and c4, and cut into them toward the main normal fault, is a similar 20-30 cm-thick layer of alluvium (al3a, al3b, al3c) and colluvium (c3). The alluvial facies of this younger stratiform deposit is composed of three subunits; al3a (soft, moderately-sorted pea gravel), al3b (poorly sorted small pebble gravel), and al3c (moderately-sorted pea gravel). These deposits are generally softer, better sorted, and more clast-rich than unit al4. Unit al3a appears to have eroded into and removed either unit al4 or c4 adjacent to the main normal fault. The lens shape and moderate sorting of units al3a and al3c, plus their occurrence at the structurally lowest part of the half-graben, suggest that they represent local channel deposits that trend parallel to the trough axis. These units also dip about 20^{o} toward the fault, except adjacent to the main fault plane where they dip 10^{o} north, probably from fault drag.

The next four units form two pairs of deposits dissimilar from the alluvium-colluvium facies described previously. Unit s2AC (slopewash with AC soil horizon development) and overlying unit c2A (scarp-derived colluvium with a buried A horizon) form a coarsening-upward sequence. Unit s2AC is a light to medium gray silty sand with few clasts and contains no visible stratification (although weak stratification could have been obscured by the overprinting of organic matter). The relative absence of clasts argues against it being colluvium, particularly scarp-derived colluvium. Its occurrence at the structural low point, and the lens-shaped cross-section, suggest it might have been deposited by running or ponded water. However, its lack of stratification and small gravel means that it is probably a distal sheetwash or slopewash deposit that accumulated in the topographic low point of the half graben,

perhaps in temporarily ponded conditions, such as a temporary sag pond. This unit grades upwards into a more poorly-sorted, clast-rich unit interpreted as scarp-derived colluvium. Clast long axes tilt north, toward the low point of the graben, as if they were deposited on a slope that ran from the footwall to the hanging wall. This dark gray deposit is abruptly truncated at its top by lighter, softer material (described next), but the dark color grades downward into unit s2AC. This pattern is consistent with unit c2A containing a buried soil A horizon, the AC horizon of which extends down into unit s2AC. Because this deposit pair is more lenticular than tabular it is difficult to state whether it has been backtilted toward the fault, as were the underlying deposits. The top of unit c2A dips north at about the same angle as the overlying ground surface. If these two surfaces were both produced by colluvial transport, then it argues that neither units c2A/s2AC or units c1AC/s1Cox have been significantly backtilted toward the fault.

The upward transition from alluvial channel deposits (units al3a-c) to sag pond/colluvial wedge deposits (units s2, c2, s1, c1) suggests that the trough was suddenly deepened here, and became for the first time a closed topographic depression. Prior to that time, the channel deposits of units al3 and al4 suggest that ponding was not occurring at the trench site. After the formation of topographic closure and the influx of slopewash to its nadir, gravelly colluvium began moving down into the trough from the footwall. This scenario implies that considerable new relief was created across the main normal fault prior to the deposition of unit s2AC, and a free face was created over the main normal fault that was large enough to begin shedding colluvium into the trough. Prior to this time there is no evidence of scarp-derived colluvium being deposited here.

The youngest two deposits form a pair similar to the c2A/s2AC pair. The lower member, unit s1Cox, is also a clast-poor, lens-shaped deposit of silty sand and is interpreted as distal slopewash deposited in the low point of the trough, perhaps in ponded conditions. This deposit is weakly oxidized to a pale yellow color but does not contain any visible organics from the surface soil, hence we give it the soil horizon designation Cox. The overlying unit c1AC is a medium-gray, poorly-sorted, soft, gravelly colluvium with downslope fabric of clasts. These clasts can be traced toward the main normal fault plane (top of F5), where it appears that unit c1AC is in depositional contact with the footwall, rather than in fault contact as are all subjacent units. The medium gray color is darkest directly below the ground surface and lightens downward, consistent with a decreasing amount of soil organic matter below the surface. The gray color is not dark enough to be termed a good A horizon, so we term it a transitional AC horizon. The only material overlying this unit is the 5-10 cm-thick duff layer, composed of pine needles.

3.4.2.2 Deposits On the Footwall

The unconsolidated deposits on the footwall of the main normal fault are much thinner (0.5-0.75 m thick) than the sequence beneath the trough axis (1.5 m thick). In addition, the footwall sequence does not contain the numerous lens-shaped channel or sag pond deposits seen beneath the trough; instead, the four units defined form more laterally extensive sheets. The two older units (c4 and c2-3AC) are poorly-sorted, gravelly silty sands, with unit c3 being considerably harder and denser than c2-3AC. We correlate unit c4 here to unit c4 in the trough sequence, based in similarity in color, texture, hardness, density, and being the oldest unconsolidated deposit in both areas that lies directly upon Pelona Schist bedrock. The deposit dips about 20^{o} south.

The correlation of unit c2-3AC with the trough sequence is less certain. Partly, our age assignment of 2-3 for this deposit is dictated by the inferred age of the underlying c4 colluvium and the overlying very loose and young sag pond deposits (s1 and s1AB, described next). The colluvium on the footwall that occupies the space between units c4 and s1 must represent the same span of time as represented by the trough units between c4 and c1AC/s1Cox. In the trough we had defined two ages of units in this time interval (al3/c3 and s2/c2), so we must define the intermediate deposit on the footwall as spanning both time intervals, as signified by c2-3AC. The AC designation represents the fact that this colluvium, which probably accumulated slowly on this uplifted and rotated fault block, has been near enough to the ground surface to receive surface-derived organic material. However, the amount of organic material that accumulated here on this topographic high is not enough to deserve true A horizon status, hence the transitional AC horizon designation. This deposit dips about 10^{o} south.

The youngest deposit on the footwall is a massive, lens-shaped deposit of clast-poor silty sand, up to 25-30 cm thick at the south end of the trench but pinching out to the north. This fine-grained deposit lies in a very subtle, nearly circular topographic depression that marks the termination of one fault strand in a stepover zone (described in Sec. 3.4). We interpret it as a sag pond deposit composed of distal sheetwash that settled out in temporarily ponded conditions. The lower part of the unit is unaffected by pedogenesis, so is simply named unit s1. The upper part of the deposit has been affected by surface soil formation, with medium gray colors from organic matter combined with a weak, subangular blocky soil structure reminiscent of cambic B horizon development (e.g. Birkeland, 1999). We term this transitional soil horizon s1AB.

3.4.2.3 Deposits Beneath the Northern Boundary Scarp

The deposits underlying the northern boundary scarp are dominantly crack fills (units cf1, cf2, and cf3). The largest crack fill area (surrounding fault F9) is flanked by more tabular deposits of colluvium that underlie the ground surface. To the south, the colluvium appears to be a continuation of unit c1AC, and this colluvial deposit pinches out on the toe of the northern boundary scarp. North of fault F9 the surface is underlain by a slightly denser colluvium with a better-developed soil profile than the weak AC profile found on unit c1; this parent material is correlated with units 2 and 3 in the trough axis.

3.5 Geochronology (see Table 1)

Six radiocarbon samples were collected from this trench but only four were dated due to lack of funds. Samples B-139497 through B-139499 were charcoal and are in correct stratigraphic order. In contrast, sample 139500 was a bulk soil sample from a weakly organic (Cox) soil horizon developed on slopewash (unit s1Cox). This sample lies above the 3 charcoal samples but yields a date older (1705-1855 cal yr. BP) than the oldest of the three charcoal samples (1055-1165 cal yr. BP). Sample B-139500 also yielded the largest standard deviation of all four samples. We interpret the fine organic carbon dated in sample B-139500 to have been deposited along with the sediment, by slopewash deposition following the Most Recent faulting Event (MRE). This faulting event presumably created small scarp faces above the fault that exposed soil c2-3AC on the footwall, and some of that soil was then eroded and redeposited into slopewash unit s1AC in the low point of the graben. Thus, we believe much of the carbon dated in B-139500 was recycled from soil horizon c2-3AC, and does not accurately represent the age of unit s1AC, and thus the MRE.

Instead, we use the three charcoal samples to constrain the date of the MRE. The youngest sample (B-139499) is from the youngest fissure fill (cf1). This fissure cuts soil horizon

Table 1. Radiocarbon samples collected and dated in this study.

Radiocarbon sample data from 1999 S. California sackungs					Lab. No.	Lab. C-14 age (C-14 years BP)	Calibrated Age (+/- 1 sigma, calendar years BP)	Event Constraint
Blue Ridge trench					Beta-xxxxxx			
Field No.	Unit	X coord.	Y coord.	Material				
BR-C1	c2A	6.8	0	A horiz.				close max. on Z
BR-C2	s2AC	5.5	-0.2	charcoal	139497	1180+/-40	1055-1165	between Z and Y
BR-C3	s2AC	5.6	-0.1	charcoal				between Z and Y
BR-C4	c2A	6	0	charcoal	139498	860+/-40	725-790	close max on Z
BR-C5	cf1	7.8	0	charcoal	139499	230+/-30	285-300	close min on Z
BR-C6	s1Cox	6	0.1	Cox bulk	139500	1840+/-60	1705-1855	close min. on Z
Upper Lytle Creek Ridge trench								
LC-C1	3AC	7.8	-1.45	charcoal	139501	3780+/-30	4095-4170	min. on X
LC-C2	cf1	1.2	-0.5	A horiz.				close min. on Z
LC-C3	cf3	1.4	-0.8	A horiz.				close min. on X
LC-C4	cf1	6.5	-1.3	A horiz.	139502	3060+/-40	2760-2851	close min. on Z
LC-C5	cf2	6.1	-1.3	A horiz.				min on X
LC-C6	3Ab2	6.9	-1.5	A horiz.	139503	3600+/-40	3432-3533	close max. on X
LC-C7	2Ab1	7.1	-0.9	A horiz.	139504	2440+/-50	1993-2125	close max on Y
LC-C8	1AC	7.25	-0.7	A horiz.	139505	1270+/-40	746-867	close max. on Z
Kagel Mountain trench								
KM-C1	5bA1b2	23.2	-3.4	charcoal	139508	1940+/-60	1830-1945	close min on Z
KM-C2	3a	22.5	-5	charcoal	139506	2790+/-40	2845-2935	close min on Y
KM-C3	2	22.2	-5.05	charcoal	139507	9460+/-40	10655-10725	close max on Y
KM-C4	3b	23.4	-4.55	charcoal				between Z and Y
KM-C5	4b	variable	variable	charcoal				max on Z
KM-5a	4b	variable	variable	charcoal				max on Z
KM-C6	4bACb3	24.2	-3.8	charcoal	139509	2310+/-70	2315-2355	close max. on Z
KM-C7	6ACb1	24.65	-3.2	charcoal				far min. on Z
KM-C8	7d	20.5	-3.1	charcoal				far min on Z

Instead, we use the three charcoal samples to constrain the date of the MRE. The youngest sample (B-139499) is from the youngest fissure fill (cf1). This fissure cuts soil horizon c2A (which underlies the colluvial wedge deposited after the MRE), and its fissure fill (unit cf1) is also overlain by unit c1AC. Thus, the cross-cutting and stratigraphic relationships suggest that the fissure was created during the MRE, and was filled before the toe of the colluvial wedge advanced outward from the scarp 4 m away and buried it. The C-14 date of 285-300 cal. yr. BP must therefore post-date the MRE, by the amount of time necessary to fill the open fissure.

The soil that underlies the MRE colluvial wedge yielded dates of 725-790 cal. yr. BP (B-139498) and 1055-1165 cal. yr. BP (B-139497). The younger date is closer to the event horizon (the s1AC/c2A contact) so constitutes the tighter age constraint. Both of these dates predate the MRE by some unknown amount of time. Without correcting the dates for distance from the event horizon, we can say that the MRE occurred before 285-300 cal. yr BP and after 725-790 cal. yr BP.

The oldest valid charcoal date comes from the older, slopewash part of colluvium deposited after the Penultimate Event (PE). This sample (B-139497) postdates the PE by the amount of time required to deposit 30 cm of slopewash in the low point of the graben; however, it may also be contaminated by older recycled carbon as was slopewash unit s1AC. Therefore, the age of 1055-1165 cal. yr BP constitutes only a loosely limiting minimum age for the PE.

3.6 Interpretation

The sequence of displacement events and depositional events was reconstructed through the use of a series of simplified diagrams based on trench wall relations (Fig. 7). The key geometric relationships used to draw these diagrams are: 1) cross-cutting relationships between fissure fills and stratiform deposits, 2) superposition of stratiform deposits, 3) fault truncation of units older than c1, 4) depositional contact of unit c1 with the buried fault free face, 5) interpretation of c2 and c1 as scarp derived colluviums, based on location, geometry, and clast fabric, 6) assumption that free face height was roughly twice the maximum thickness of colluvium shed from it, 7) change of depositional style from alluvium of al3 and al4, to sag pond deposits of s2 and s1, indicating closure of this part of the trough. Although the diagrams have been simplified geometrically (e.g, the main normal fault zone is represented as one fault rather than two), the key relationships mentioned above are correctly portrayed as they exist today (for more details, see the figure caption).

The early evolution of the trough appears to be dominated by fissuring rather than faulting. For example, the event that created the cf4 fissure (Event 1) did not result in the formation of a colluvial wedge. Instead, the cf4 fissure is overlain by alluvium (al4). This suggests that the earliest fissuring event only created enough of a topographic depression here to funnel local runoff. The sedimentology of unit al4 does not suggest ponded conditions, suggesting that the trough was not a closed depression as it is today. The second deformation event (Event 2) was also accompanied by fissuring (creation of cf3 fissures that offset unit c4), but also must have been accompanied by enough slip on the main normal fault to create the 0.3 m of accommodation space into which units al3 and c3 were deposited. However, there is no trace of a scarp-derived colluvial wedge being shed into the trough at this time. The similar dips of units al3/c3 and al4/c4 indicate that there was no significant tilting of the hanging wall between their deposition. Thus, almost all of the 20^{o} of present backtilt of these units occurred during the two later faulting events.

After the deposition of units al3/c3 the style of deformation changed. In two faulting events (inferred from two scarp-derived colluvial wedges), > 2 m of net slip occurred on the main fault, and the hanging wall (as well as the footwall) were rotated 20^{o} counterclockwise (looking west). These two large-displacement events formed a trough that was a closed depression at this site, and deposition since that time has been dominated by sag pond and scarp-derived sediments rather than by lenses of alluvium/colluvium. This interpretive sequence suggests that displacement at the site may be increasing with each successive event. Such a trend would be expected if each successive gravitational failure event brings the slope closer to landslide failure, such as has occurred at many other locations of the north flank of Blue Ridge.

Fissuring at the trench site is distributive, occurring across the entire ridge where trenched. Not all fissuring is concentrated near the main failure planes (faults F5 and F6) and some of the fissuring may reflect events other than the four identified. In addition, the width of crack fills (faults F1, F7-10) indicates that a large amount of extension has occurred across the ridge. Although the net extension is difficult to measure, the width of cf3 at F9 suggests at least 50 cm of extension in a single deformation event. This value is consistent with observations made after the Loma Prieta earthquake (e.g., Hart et al., 1990; Spittler and Harp, 1990; Ponti and Wells, 1991). This mixed deformation style of normal faulting, hanging wall rotation, and pure extension is important for the design and placement of structures on ridge crests.

If we compare the ages of the MRE and PE here with the paleoearthquake chronology of the San Andreas fault, which lies at the base of Blue Ridge, we see that the dates do not correlate uniquely with any one paleoearthquake (Table 2). An MRE between 285 and 790 cal. yr BP (1-sigma range) could correlate with either the AD 1480 or AD 1346 earthquakes dated by Sieh et al (1989) and Fumal et al (1993). Conversely, the MRE may not be related to any paleoearthquake; the dating is too "loose" to tell. It is tempting to correlate the PE (older than 1055-1165 cal. yr BP) with the AD 797 event on the San Andreas fault, but again, the dating constraints are too loose to be convincing. All we can say is that earthquakes did occur on the San Andreas fault within the time limits of the MRE and PE.

Table 2. Comparison of paleoearthquake dates from the San Andreas fault (Sieh et al, 1989) to C-14 dates from the Blue Ridge trench.

Earthquake Dates (cal. yr. A.D)	Earthquake Dates (cal. yr. BP)	Dates from Trench (cal. yr. BP)
1857	93	
1812	138	285-300 (postdates MRE)
1480	470	
1346	604	
1100	850	725-790 (predates MRE)
1048	902	
997	953	
797	1153	1055-1165 (postdates PE)
734	1216	
671	1279	

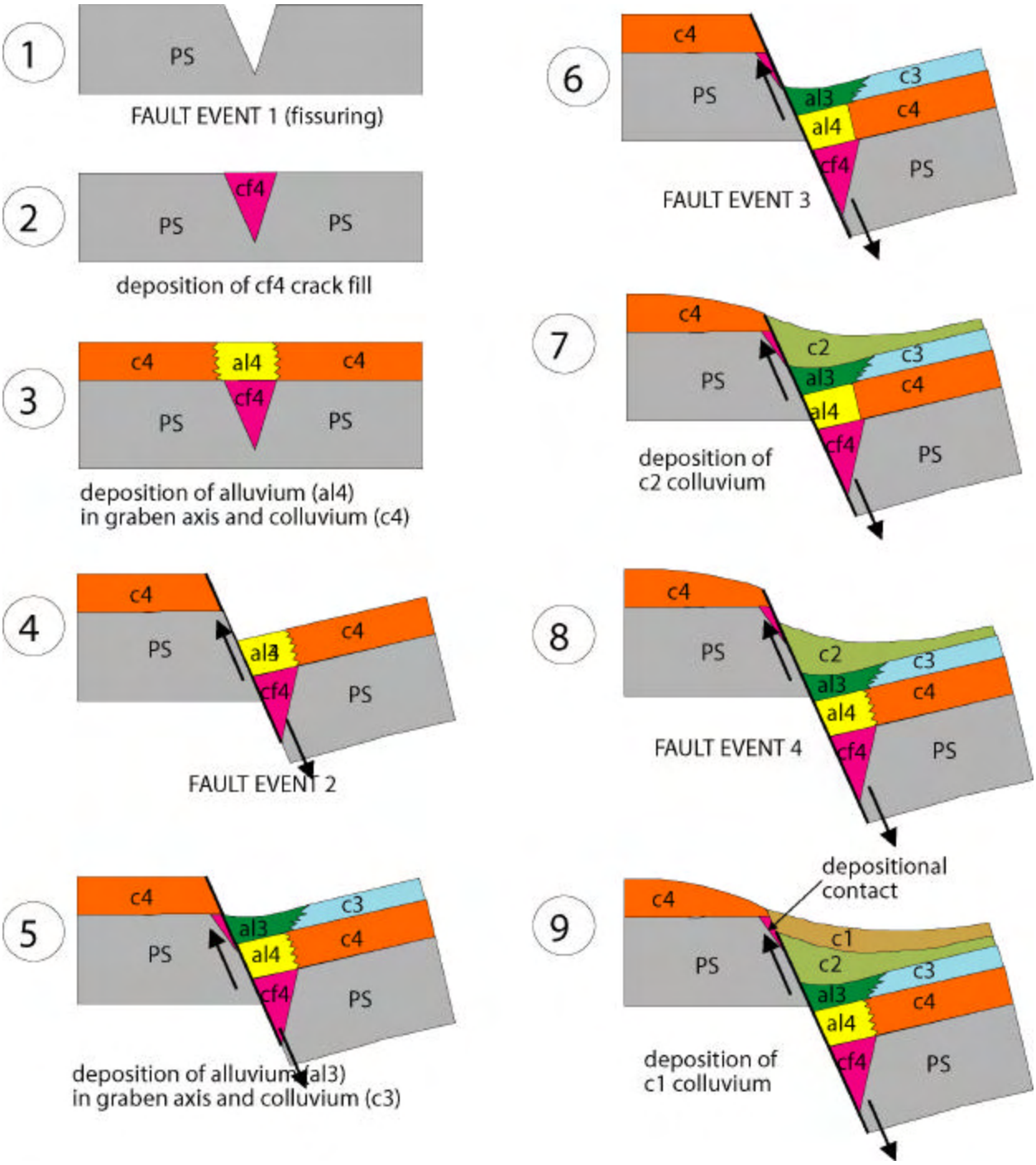

Fig. 7. Inferred sequence of events on the main normal fault zone that formed the Blue Ridge sackung. Step 1 is the earliest stage and Step 9 is the present stage. In these diagrams the main normal fault zone (F5 and F6) have been simplified to a single fault plane. Rotation of the hanging wall is shown, but not that of the footwall, and small footwall faults are also omitted. The amount of displacement shown in Steps 4, 6, and 8 is somewhat arbitrary, not to scale, and is only meant to show that Fault Events 1 and 2 had small displacements, too small to create either a free face high enough to induce significant scarp-derived colluviation, or to rotate the hanging wall >5^{o}. In contrast, Fault events 3 and 4 accounted for most of the 20^{o} backtilting of the hanging wall, and produced free faces which shed units c2 (represents units s2AC and c2A) and c1 (represents units s1Cox and c1AC).

4. UPPER LYTLE CREEK RIDGE TRENCH

4.1 Location and Local geology

The Upper Lytle Creek Ridge trench was located on the summit of Upper Lytle Creek Ridge at 1622 m elevation, about 1.5 km south of the Sharpless Ranch and the trace of the San Andreas fault (Fig. 8). The trench site is easily accessed by Forest Road 3N31 (also called the Sheep Creek Truck Road), via a short dirt track that diverges from the graded road and travels east along the firebreak. The most direct route to the site is to drive up a poorly-maintained Forest dirt road from just west of the Sharpless Ranch to the crest of Upper Lytle Creek Ridge; 4 wheel drive is recommended.

Upper Lytle Creek Ridge is a linear, 400-500 m-high ridge (Fig. 9) that lies between the San Andreas and Punchbowl/San Jacinto faults (Morton et al., 1991) and parallels their strikes (N55W). According to Morton and Sadler (1989, p. 312) most of the ridge is "underlain by a relatively high grade, upper greenschist to lower amphibolite facies, coarse-grained schist, located between the Punchbowl (PBF) and San Andreas (SAF) fault zones. Most of the schist is the muscovite-bearing variety; greenstone is also locally common. The foliation strikes almost parallel with the [Lone Pine] canyon, dipping southward into the ridge."

4.2 Geomorphology

The crest of Upper Lytle Creek Ridge is anomalously wide and hummocky, and is cut by numerous ridgetop troughs, depressions, and uphill-facing scarps along its entire length (Fig. 10). Morton and Sadler (1989) mapped numerous landslides on both flanks of Upper Lytle Creek Ridge, and interpreted most of the ridgetop scarps and troughs as the heads of these landslides. They stated " Again, landsliding within the Pelona Schist takes on atypical aspects. The distal part of nearly every [tributary] ridge has moved by landsliding and/or deep rock creep (sagging), towards the floor of Lone Pine Canyon as well as laterally into inter-ridge canyons. This type of landsliding results in the formation of morphologically distinctive, blunt-nosed lower ridges with flattened or trenched ridge tops, and common side hill trenches. Some ridges are dominated by trenches with no expression of a landslide deposit. The trenches appear to form by lateral displacement, with backwards rotation, of ridge top material towards the free face of the inter-ridge canyons. Side hill trenches form where the head or scarp of the landslide is on the opposite side of the ridge from the toe of the landslide."

They further speculate "The abundance of side-hill and ridge-top trenches in such close proximity to the San Andreas [fault] suggests a causative relationship between this type of landslide and shaking from earthquakes. The side-hill and ridge-top trenches seem to be the result of the repeated occurrences of shattered ridge tops. Shattering results from focusing energy near the top of a ridge during an earthquake. Shattered ridge tops have now been described for a number of southern California earthquakes...."

We placed our trench across a broad 100 m-long, 30 m-wide depression that appeared to have about 1 m of topographic closure (Fig. 11), although some of this closure was created by spoil from bulldozing of the ridgetop firebreak several decades earlier. Both the northern and southern boundary scarps of this depression have gentle slopes, but the northern scarp is higher (ca. 2 m) than the southern one (ca. 1.3 m). As we found elsewhere, the major normal "fault" lies beneath the smaller scarp and the larger scarp overlies a tilted and fissured block.

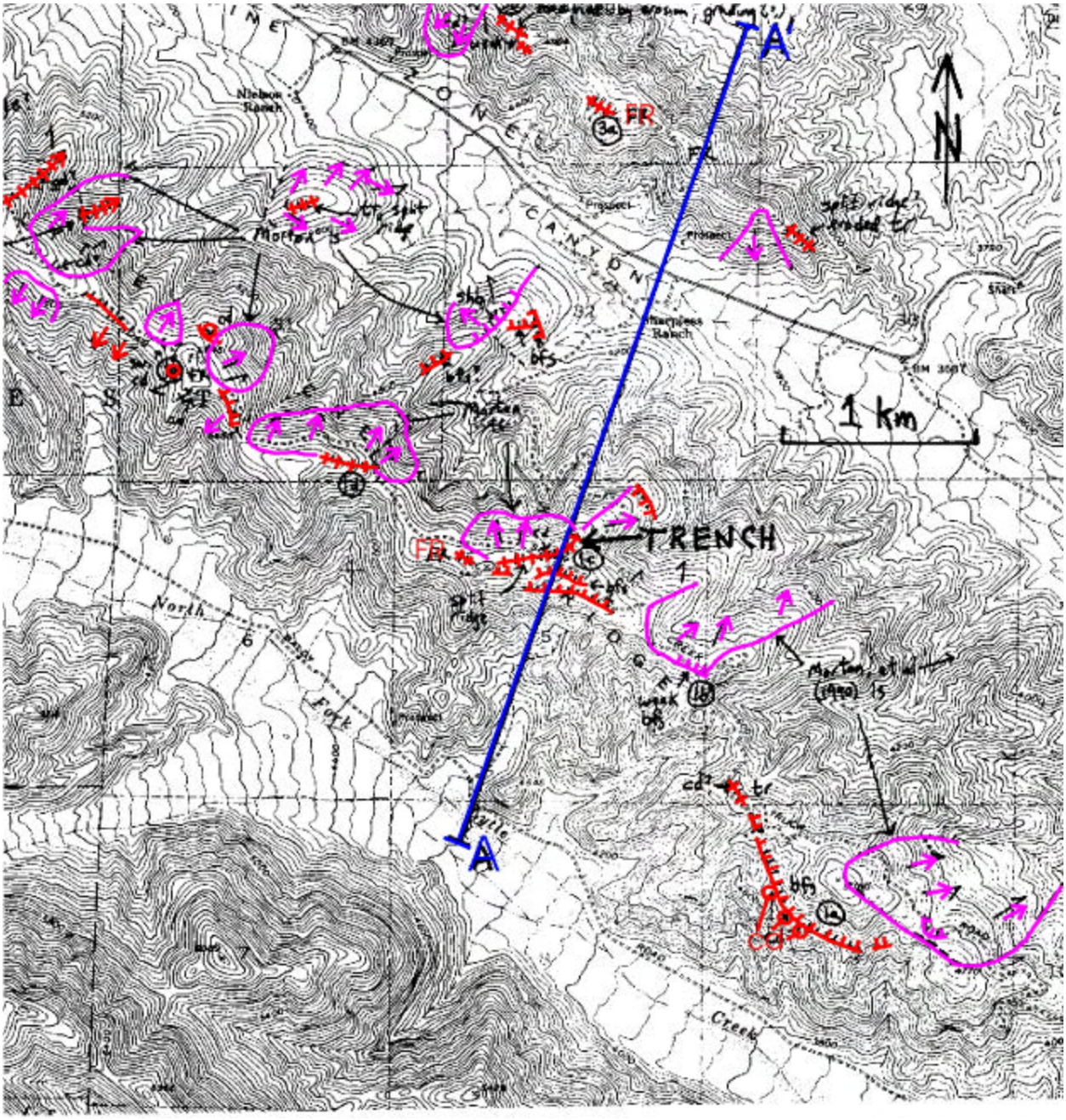

Fig. 8. Location map of the Upper Lytle Creek Ridge trench site, Telegraph Peak quadrangle. See Fig. 2 for explanation of symbols

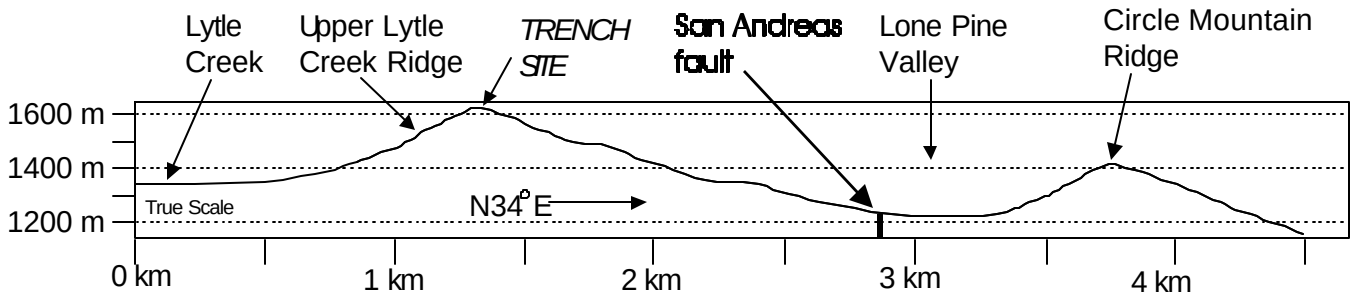

Fig. 9. Topographic profile of Upper Lytle Creek Ridge.

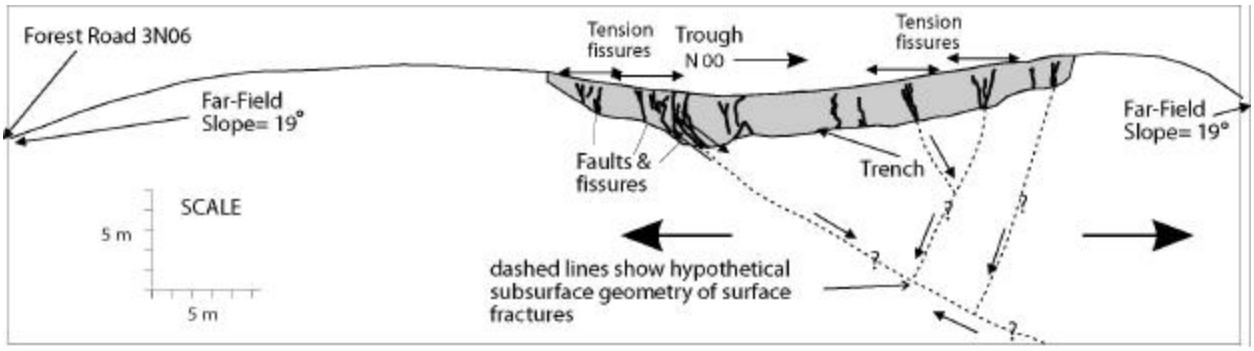

Fig. 11. Topographic profile of the Upper Lytle Creek Ridge trench site. Dashed and queried lines beneath the trench show one possible subsurface geometry for the "faults" observed in the trench. Large arrows indicate the general sense of N-S extension.

Fig. 10. Photograph of the site of the Upper Lytle Creek Ridge trench, looking east. The trench runs N-S (left to right) across the light-toned gassy meadow at left center, left of the dirt road (note vehicle on road, and faint yellow caution flagging outlining the trench). Mountain range in distance at upper right is the western end of the San Bernadino Mountains.

4.3 Structure

The depression we trenched is the surface expression of a south-tilted half graben (Fig. 11), bounded by a major normal "fault" on the south and a south-tilted block cut by fissures on the north. We define 10 large fractures (F1 through F10) plus a few smaller fractures with little or no vertical displacement (Fig. 12). The major failure plane (F5) defines the hanging wall and footwall of the half-graben. The footwall contains several small-displacement fractures (F1-F4), as does the tilted hanging wall beneath the northern boundary scarp (F8-F10). This geometry is very similar to that observed in the Blue Ridge trench.

The main failure plane (F5) dips 45^{o} north in its lower 1.2 m (exposed), but then curves to vertical and changes character. Total vertical displacement on F5 measured on the top of Pelona Schist bedrock is 1.6 m, an amount somewhat less than the 1.8 m depth of the depression at this point. The additional depth was created by an additional 1 m of throw on fractures F1 and F2, discussed later. The lower, 45^{o}-dipping section of F5 abuts bedrock against unconsolidated graben fill sediments (unit 2Cn), and comprises a 10-15 cm-wide shear zone in which angular, tabular schist clasts have been rotated so that their long axes parallel the shear zone. This shear zone resembles the lower part of the main normal "fault" in the Blue Ridge trench. Closer to the surface, fracture F5 juxtaposes older against younger graben fill sediments, and here the fracture becomes vertical. This abrupt change in dip probably results from the change in rheological characteristics of the faulted materials (bedrock versus graben fill). The effect of this 45^{o} change in dip is to split the fracture into two parallel strands (F5a and F5b), each of which is characterized by a large tension fissure. Fracture F5a, which is the southern and more direct continuation of F5, displays a 25 cm-wide filled fissure but only 5-10 cm of vertical displacement, as measured on the top of the oldest unconsolidated unit (3Cn). Fracture F5b contains a smaller fissure fill that does not continue widening toward the surface, but instead pinches out upward and transforms into a narrow fault plane. Throw across this near-vertical fault is about 0.7 m, as measured on the top of unit 3Cn. Fracture F4 is also related to this main zone of normal faulting, because it coincides with a 0.7 m downthrow of intact schist (unit PS). The area of exploded schist (ES) between fractures F4 and F5 is extensively sheared and many shattered pieces of rubble have been rotated parallel to fracture F5.

The footwall of fractures F4-F5 contains three deformation zones that are mainly tension fissures. All three of these fractures underlie the southern boundary scarp. Fracture F3 contains fissure fills of at least two ages but displays little or no vertical displacement. Kinematically it is probably more closely related to extensional fractures like F4, F5a, and F5b than to the other fractures in the footwall. Fractures F1 and F2 are also extensional features containing fissure fills of 2-3 ages, but each also displaces the top of bedrock down toward the trough axis (by 0.4 and 0.6 m, respectively).

The hanging wall underlies the northern boundary scarp, and comprises a south-tilted block of bedrock with a thin layer of old colluvium on it. The three major deformation zones in the hanging wall (F8-F10) have small displacements compared to fractures F1-F5, and probably reflect local adjustments of this slab to rotation towards the main normal "fault". Fracture F8 is a 30 cm-wide tension fissure that may have a small component of down-to-the-north throw. Fractures F9 and F10, both with down-to-the-south throw, look like typical normal faults without significant extension and development of open fissures. Fracture F9 experienced about 0.6 m of throw, which was enough to generate a small colluvial wedge (unit 4c). The bedrock block between fractures F9 and F10 has been rotated about 5^{o} to the north. Fracture F10 is a smaller-scale version of F9, with about 15-20 cm of throw.

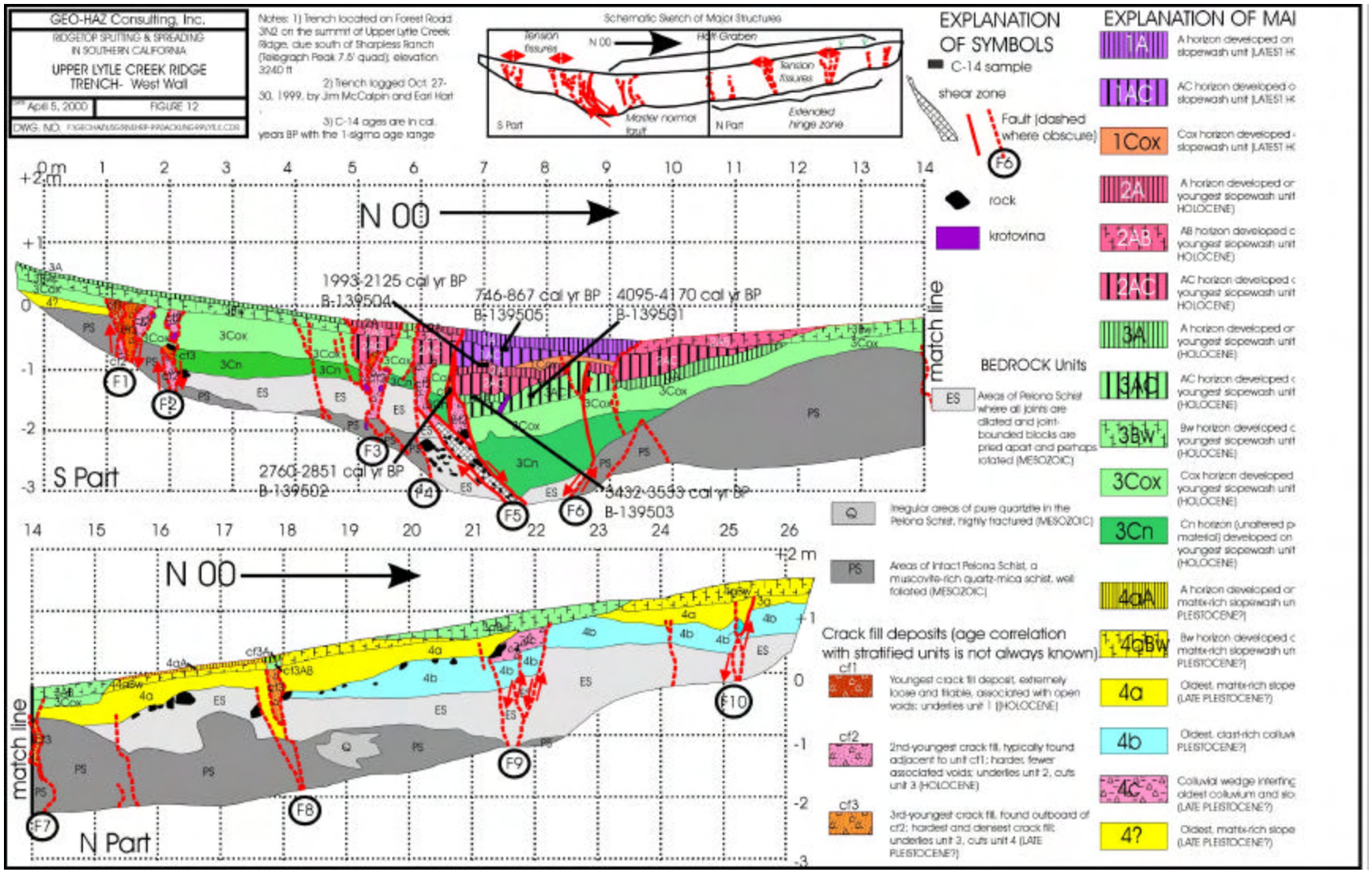

Fig. 12. Log of the Upper Lytle Creek Ridge trench. These two fractures and the intervening tilted block look like domino-style faults formed by northeast-southwest extension. This extension was then accommodated by normal slip on the fractures and clockwise rotation of the intervening block (as viewed on the log). Fractures F9 and F10 appear to be antithetic to F5.

4.4 Stratigraphy

We distinguished 3 bedrock map units and 20 unconsolidated map units in this trench. Criteria for defining units and the techniques of logging follow those described by McCalpin (1996b).

4.4.1 Bedrock Map Units

We divided the Pelona Schist into 3 mapping units. Unit PS represents areas of relatively intact schist that exhibits a consistent foliation. Although some joints may be dilated, the schist blocks have not been rotated out of position. The joints themselves do not contain a large amount of unconsolidated fill. Unit Q represents a pocket of pure vein quartz within the schist. This quartz was extremely shattered on a 0.5-1 cm spacing and fell piece-by-piece out of the wall over a period of several days. Map unit ES is "exploded schist". This unit represents areas of Pelona Schist where schist blocks have rotated out of their original orientation and now display various foliation directions. The joints are partly to wholly filled with smaller schist rubble but this
rubble does not contain any colluvial or slopewash material derived from Quaternary unconsolidated units; it is all crushed schist. These areas look like the rock was blasted with explosives ("exploded") and all the joints were opened enough that schist blocks could rotate.

4.4.2 Unconsolidated Units

The unconsolidated deposits exposed in the trench form three local stratigraphic sequences deposited in three different structural domains. These domains are: 1) footwall of the main normal "fault", between 0 and 6 m on the log horizontal scale; 2) hanging wall beneath the trough axis, between 6 and 13 m; and 3) hanging wall beneath the northeastern boundary scarp, between 13 and 26 m. The boundary between the latter two sequences is a bedrock high, where the unconsolidated deposits have been thinned by erosion and many units disappear. Below, we describe each stratigraphic sequence separately.

4.4.2.1 Deposits Beneath the Trough Axis (6-13 m)

Unconsolidated deposits are thickest beneath the trough axis (2.2 m) and are divisible into the most units. The oldest deposit lies directly upon exploded schist and is a 1.5 m-thick massive, slightly gravelly, silty sand (unit 3), which contains four soil horizons (from top to bottom, 3A, 3AC, 3Cox, 3Cn). Despite our best efforts, we were unable to further subdivide this thick unit (it comprises 70% of graben fill thickness) into more than one parent material. There are no textural or sedimentologic breaks (stone lines, etc.), nor structural indicators (upward-terminating fractures, angular unconformities) that would indicate that this deposit was deposited in more than one episode. Given the narrow width of the deep structural "pocket" beneath the trough axis, it is conceivable that this material was washed relatively rapidly into the narrow trough by local sheetwash. There are no sedimentary structures or textures indicative of ponding or subaqeous deposition (i.e., true sag pond conditions). The top of unit 2 dips 10^{o} toward the main normal fault zone.

The top 30 cm of unit 3 is a buried soil (horizons 3A and 3AC), and this soil is overlain by a lens-shaped deposit of sandy slopewash (unit 2) that is very similar in texture and lack of bedding to unit 3. Unit 2 has been subjected to sufficient pedogenesis that a thin 2A horizon and a thicker 2AC horizon now extend through its entire thickness. The bottom of parent material 2 lies on the 10^{o}-dipping surface

of unit 3, but the top of unit 2 is nearly horizontal. This implies that the tilting of unit 3 largely predates unit 2.

The youngest parent material adjacent to the main normal fault is unit 1. Like unit 2, this unit has been engulfed by soil formation associated with the modern ground surface, and is divided into units 1A and 1AC. Units 1A and 1AC occupy the lowest part of today's trough and clearly constitute the youngest deposits in this depression. Given this youth, the southern, vertical-to-overhanging contact of units 1A/1AC against units 2A/2AB/2AC is puzzling. This contact appears to be the extension of fault F5b and can be traced to the modern ground surface as the contact between the very soft parent material 1 and the slightly harder parent material 2. However, if this is a true fault contact it poses a problem in interpretation, because we interpret parent material 1 as the slopewash that filled in the accommodation space created by the last major faulting event in this graben. In other words, parent material 1 should be younger than the most recent faulting event (MRE), so it cannot itself be faulted. However, if the contact is depositional why does it overhang? This dilemma is discussed further in Sec. 4.6.

4.4.2.1 Deposits On the Footwall (0-6 m)

The unconsolidated deposits on the footwall are primarily units 3Cn and 3Cox. These units are identical to the same units just described beneath the trough axis. However, on the footwall the upper part of unit 3 has remained exposed to surface soil processes since its deposition, rather than being buried by younger sediments as in the trough axis. As a result of this longer exposure the upper part of unit 3 has developed a cambic B horizon (3Bw) beneath the thin A horizon (unit 3Ab). This Bw horizon also extends through the intermediate-age crack fills (unit cf2) that are younger than unit 3 (Fig. 12).

South of faults F1 and F2 the unconsolidated deposits thin from 1.3 m to 0.5 m. The attenuated stratigraphic section at the southern end of the trench is composed of the same upper three soil horizons as elsewhere on the footwall (3Ab, 3Bw, 3Cox), with an additional very dense but thin colluvium (unit 4?) overlying schist. This colluvium may be the same as the old colluvium that is discontinuously present atop bedrock in the northeastern half of the trench (described next).

4.4.2.3 Deposits on the Hanging Wall (13-26 m)

The northern half of the trench comprises the tilted hanging wall structural block. The rather thin unconsolidated deposits that overlie bedrock in this area are denser, more poorly sorted, and more clast-rich deposits than the softer, sandier deposits in the southern half of the trench. The oldest unconsolidated deposit (unit 4b) directly overlies schist bedrock (PS and ES), and is a very hard, dense, buff-colored gravelly sand with no visible stratification or sedimentary structures. The texture of the deposit suggests it is residuum or locally-derived colluvium. Unit 4b is dismembered by normal faults F9 and F10 and has been eroded from the top of the F9 footwall between F8 and F9.

The next youngest deposit (unit 4a) has a buff color, hardness, and density similar to that of unit 4b, but contains virtually no clasts. In texture it somewhat resembles the clast-poor slopewash units farther south in the trench (e.g, units 1-3), but its hardness and density imply that it is older than unit 3 beneath the trough. The bottom contact of unit 4a truncates unit 4b at fault F8, south of which unit 4a rests directly on schist bedrock. Given the similar density and hardness of these two units, we infer that this 4a/4b contact is a facies contact between deposits of similar age, rather than an erosional contact of younger slopewash into much older colluvium/residuum.

Unit 4c overlies unit 4b on the hanging wall of fault F9 and grades laterally into unit 4a. The shape of this deposit, its location, and the orientation of clasts (long axes dip away from the fault) suggest this unit is a colluvial wedge shed from a free face created by F9. The age of this faulting event is clearly younger than unit 4b, and is probably younger than some of unit 4a, because that unit is erosionally truncated on the footwall of F9. For example, if all of unit 4a was younger than the faulting, then it should drape over the fault zone rather than being truncated. However, the fact that 4c seems to grade into 4a on the downthrown side of F9 implies that faulting occurred during the deposition of unit 4a, rather than after it. Perhaps the best compromise interpretation is that the faulting on F9 occurred during the deposition of unit 4a.

Over about 60% of the length of the hanging wall unit 4 is at the ground surface and carries an A horizon (4aA) and/or Bw soil horizon (unit 4aBw). The degree of Bw horizon development is similar to that contained in unit 3Bw in the southern part of the trench. However, in about 40% of the hanging wall length the ground surface is underlain by a softer, less dense colluvium (units 3AB, 3aBw) that overlies unit 4a. The southern unit (3AB) is physically connected to the stratigraphic sequence beneath the trough, so its age correlation is well supported. Unit 3aBw forms an isolated lens above fault F9 and is only assigned its age designation of "3" because: 1) the unit clearly overlies and truncates units 4a and 4b, so must be younger, 2) it is much softer than units 4a and 4b, and 3) it is old enough to carry a Bw soil horizon, so must be older than unit 2 in the trough sequence, because that parent material only reaches a maximum development horizon of AB, rather than a full-fledged Bw.

4.5 Geochronology

The radiocarbon samples collected from stratigraphic units beneath the trough axis are in correct stratigraphic order, except for the sample from the crack fill unit cf1. Furthermore, the four samples define a nearly linear deposition rate of 0.3-0.35 m/kyr, with ages ranging from 746-867 cal yr BP (middle of unit 1) to 4095-4170 cal yr. BP (unit 3AC). Extrapolation of the deposition rates to the base of the trough fill predicts an age of ca. 8.5-10 ka for the creation of the trough. However, there are no buried soils in the lower 1.5 m of the trough fill, so perhaps the deposition rate in this part of the trough fill was more rapid than 0.3-0.35 m/kyr.

The age of unit cf1 (2760-2851 cal yr. BP) is not consistent with the cross-cutting relationships mapped on the trench log. According to the log, crack fill unit cf1 clearly truncates unit 2AC, so must be younger than 1993-2125 cal yr. BP, yet its C-14 age is older. Secondly, crack fill unit cf1 is mapped as juxtaposing unit 2 in the footwall with unit 1 in the hanging wall. If this contact is a fault contact, it implies that unit cf1 formed after the deposition of unit 1, which has an age of 746-867 cal yr BP. Finally, if the C-14 age of unit cf1 is taken as correct, then this crack fill unit is intermediate in age between unit 3Ab2 and unit 2Ab1, both of which it truncates.

The answer to this dilemma may be the source of the organics in unit cf1 crack fill. The probable source of this organic crack fill is a thin slab of units 2A/2AB/2AC falling down into the fissure from the footwall. Such a thin slab would disaggregate once it fell into the fissure and the organic materials from the 3 component soil horizons would become mixed. The upper part of the thin slab (unit 2A) would have contained organics with an age of 1993-2125 cal yr. BP, whereas the lower part of the slab (unit 2AC) would have contained organics with an age somewhat younger than unit 3Ab (3432-3533 cal yr. BP). The arithmetic mean of these two ages is 2763 cal yr. BP, which is very close to the C-14 age of the crack fill (2760-2851 cal yr. BP). In other words, a slab composed of units 2A, 2AB, and 2AC, if

homogenized, and given the linear shape of the age-with-depth curve, would yield a C-14 age very similar to that of crack fill unit cf1. After this slab fell into the crack, the crack was buried by units 1A and 1AC. This scenario, however, does not explain how crack unit cf1 continues upward into unit 1AC.

4.6 Interpretation

Based on cross-cutting relationships and angular unconformities, at least 3 or 4 episodes of displacement created this trough (Fig. 13). Evidence for the earliest event (W) is presence of unit 2. This fine-grained slopewash deposit could not have been deposited on this ridgetop without the existence of a swale or depression. The southern boundary of this depression could have been faults F1 and F2, which mark the southernmost extent of thick slopewash deposits. The northern side of the depression was probably formed by slight southward tilt of the hanging wall block into faults F1 and F2. Extrapolation of deposition rates from the upper half of the trough fill to its base implies that this initial trough formed ca. 8.5-10 ka.

Evidence for the next displacement event (X) is the differential thickness of parent material 3 across fault F5. This differential thickness of 0.4 m requires either that: 1) vertical displacement of 0.4 m occurred during the accumulation of unit 3, or 2) vertical displacement of 0.4 m occurred after deposition of unit 3, and the upper 0.4 m of unit 3 was eroded off the footwall. Option 2 would require that the material eroded from the footwall be deposited somewhere, most likely as a colluvial wedge in the trough. Because no such wedge exists, we prefer option 1 (Steps 1-4 in Fig. 13).

Unit 3 is 0.4 m thicker north of fault F5, but in relation to the soil horizons developed in unit 3, the differential thickness is all contained within the lowest horizon (3Cn). In other words, the upper 3 horizons (3A, 3AC or 3Bw, 3Cox) maintain about the same thickness across the fault. This geometry could be approximated in two different scenarios. In scenario A (Steps 1a-4a in Fig. 13), Fault Event X occurred during the accumulation of unit 3, and the entire soil on unit 3 postdates faulting event X. Because soil formation postdates the displacement event, and soil formation proceeds from the ground surface downward, the upper horizons would maintain roughly constant thickness across the buried fault scarp. This would leave the lowest soil horizon with a differential thickness across fault F5. In scenario B (Steps 1b-4b in Fig. 13), fault Event X occurred after the entire soil had formed on unit 3. The result of this scenario is to have a differential thickness of the upper soil horizons, and a more uniform thickness of the lowest horizon (3Cn), across fault F5. Based on this "gedanken experiment", scenario A better explains the geometry across fault F5. This means that Event X occurred well after 8.5-10 ka, but before the formation of soil horizon 3ACb2, dated at 4095-4176 cal yr. BP. A tighter age constraint is not possible because the exact location of the event horizon within unit 2 is not known.

Unit 3 and its upper soil horizons are displaced across fault F5a but do not change thickness. Also, parent material 2 is continuous north of fault F5a but is present only as isolated crack fills south of that fault. This geometry requires a younger displacement event (Fault Event Y) on fault F5a (Step 5 in Fig. 13). This event was responsible for opening up the tension fissures that are now filled with crack fill of age 2 (unit cf2), and creating the accommodation space in the trough into which unit 2 was deposited

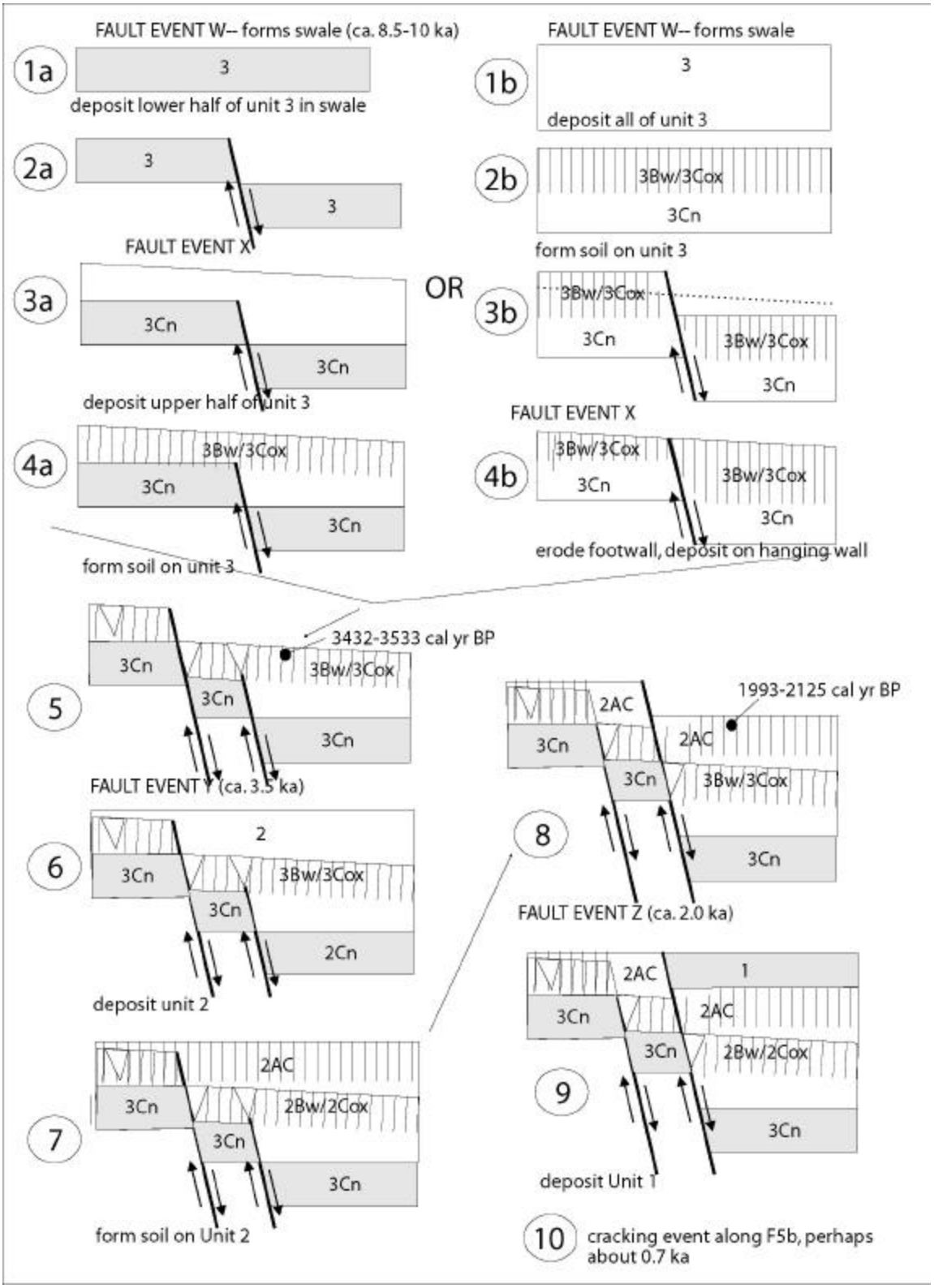

Fig. 13. Inferred sequence of events that formed the Upper Lytle Creek Ridge sackung.

(Step 6). Burial of unit 3Ab2 by unit 2 occurred about 3432-3533 cal yr. BP, which is a closely limiting maximum age for faulting event Y. Because the thickness of soil horizons in unit 2 remains constant across fault F5a, formation of all of soil 2 must postdate Fault Event Y (Step 7). Net throw across fault F5a in this event was about 0.5-0.6 m, measured on the top of unit 3; there was only minor displacement on fault F5b (described next). This faulting event was also responsible for tilting unit 3 on the hanging wall 10^{o} toward the main fault.

The youngest displacement event (Z) displaces unit 2 and its soil horizons by 0.5-0.6 m on fault F5b (Step 8). The throw across fault F5b measured on the top of unit 2 (0.5-0.6 m) is the same as that measured on the top of unit 3. This means that all the entire 0.5-0.6 m displacement of the top of unit 3 occurred during Fault Event Z, leaving none (or very little) displacement that could have occurred in event Y. Subsequent to fault event Z unit 1 was deposited in the accommodation space created in the trough axis. Burial of unit 2Ab1 by unit 1 occurred about 1993-2125 cal yr. BP, which is a closely limiting maximum age for faulting event Z.

The final event to take place is the propagation of a crack from the tip of fault F5b to the ground surface, along the depositional (?) contact between units 2 and 1. This crack creates no topographic relief on the ground surface, although bulldozers might have removed such relief during grading of the firebreak. The fill in this young crack (unit cf1) is extremely loose and friable, and open voids are present, something not observed in older crack fills. There is no scarp-derived colluvium on the north side of this crack, as would be expected if a free face had been created here. One could argue that such a wedge could also have been removed by grading, but such grading must have been minimal, because the A and Bw soil hoizons developed on units 2 and 3 were not removed. Our interpretation is that there was a post-deposit-1 cracking event. Shaking from a distant earthquake source, or some other minor disturbance may have caused this event. Judging from the upward termination of the unit cf1 fissure at the top of unit 1AC, this event may have occurred around 746-867 cal yr. BP. This time interval coincides with that of the A.D. 1100 paleoearthquake on the San Andreas fault (Table 2). However, that upward termination could also represent dieout-up (Bonilla and Lienkaemper, 1993), in which case the cracking event could be even younger.

5. KAGEL MOUNTAIN TRENCH

5.1 Location and Local geology

The Kagel Mountain trench was located on the summit of the ridge that extends east from Kagel Mountain, about 2 km east of that summit (Fig. 14). The trace of the San Fernando fault is about 5 km south of the site, and ground cracking was observed at Kagel Mountain during both the 1971 San Fernando (Barrows et al., 1974) and 1994 Northridge earthquakes (Barrows et al, 1995). The trench site is located about 2.5 km east of Pacoima Dam, which recorded horizontal accelerations of >1 g during the 1971 earthquake.

This ridge is composed of late Mesozoic (120 Ma) quartz diorite (Dibblee, 1991), correlated with the Wilson Diorite of Miller (1934). The rock is described as "gray, medium-grained quartz diorite with variations to diorite; composed of sodic plagioclase feldspar (oligoclase-andesine), biotite, hornblende, and minor quartz; massive to vaguely gneissoid; somewhat incoherent where weathered, complexly intruded by [90 Ma leucocratic] granitic rocks" (Dibblee, 1991). Foliation is mapped by Dibble as striking N30W and dipping vertical. About 100 m west of our trench on the ridge crest, Dibblee (1991) mapped a N30W-trending lens of older gneissic rocks. These rocks are described as

"medium to dark gray biotite-quartz-feldspar gneiss; hard, coherent, but much fractured; ranges from thin-layered gneiss to somewhat incoherent gneissoid quartz diorite or biotite diorite; includes small remnants of metaquartzite, biotite schist-gneiss locally containing graphite or hornfelsic gneiss, containing calc-silicate minerals (garnet, epidote, diopside, and sillimanite)".

The Kagel Mountain ridge is sandwiched between two faults. The Buck Mountain reverse fault outcrops on the south flank of the ridge about 120 m downslope from the ridge crest (i.e., the trace roughly coincides with the 3000 ft elevation contour). This fault thrusts the Mesozoic crystalline rocks of the ridge crest southward over the Saugus Formation (Pliocene and Pleistocene). The north side of the ridge is partly defined by the De Mille fault, a right-lateral splay of the San Gabriel fault (Dibblee, 1991).

5.2 Geomorphology

The part of Kagel Mountain ridge where the trench is located trends east-west, although the ridge between there and Kagel Mountain trends more southwesterly. The ridge is asymmetrical due to a large difference in base level of the streams north and south of it (Fig. 15). The south side of the ridge is drained by Buck Creek, a rather small, high-level stream that wanders over a rolling terrain eroded into the Saugus Formation. In contrast, the north side of the ridge descends to Pacoima Canyon, a major drainage that is deeply incised into the crystalline rocks of the San Gabriel Mountains. McCalpin and Hart (1999) mapped landslide deposits downslope (north) of this trench site, but could not see a direct connection between those deposits and the ridgetop scarps. However, aerial photographs show the northern flank of the ridge to be significantly benched, but no evidence of active (i.e., historic) landsliding. Due to the suspicious topography of the northern ridge flank, McCalpin and Hart (1999) classified these ridgecrest scarps as "possibly related" to deep-seated landsliding.

The trench transected a complex trough system on the ridgecrest at about 990 m elevation (Fig. 16). The main topographic feature is an east-west-trending trough about 15 m wide and 100 m long, labeled "younger graben" on Fig. 16. This trough is flanked by symmetrical scarps 1.5-2 m high and looks like a symmetrical graben. The maximum scarp slope angle on the bounding scarps (1-2 m-high) is 15-20 degrees, suggesting that each scarp is underlain by a fault, rather than one of them overlying a tilted hinge zone. The younger graben is intersected by a second, slightly shallower trough that trends nearly north-south. The intersection of these two troughs is marked by the deepest part of the closed depression, and must form some type of structural "triple junction" analogous to the junction of two oceanic spreading centers. Northeast of this intersection the east-west trough continues as a bench. This bench appears to be an older part of the east-west graben that was abandoned early in its development, perhaps after the development of the north-south-trending trough.

Our trench was originally planned to transect the middle of the younger graben and trend north-south. However, after failing to encounter true sag pond deposits and abundant organics in the Blue Ridge and Upper Lytle Creek Ridge trenches, we decided to re-orient the trench to a trend of N65E to pass through the lowest part of the closed depression. This placed the trench in a more complex structural position, with its south end crossing a right-angle bend in the southern boundary scarp, and its north end very near the end of another scarp. However, because our goal is mainly dating displacement events rather than measuring amounts of displacement, we felt that the added chance of encountering datable material outweighed the disadvantages of this alignment.

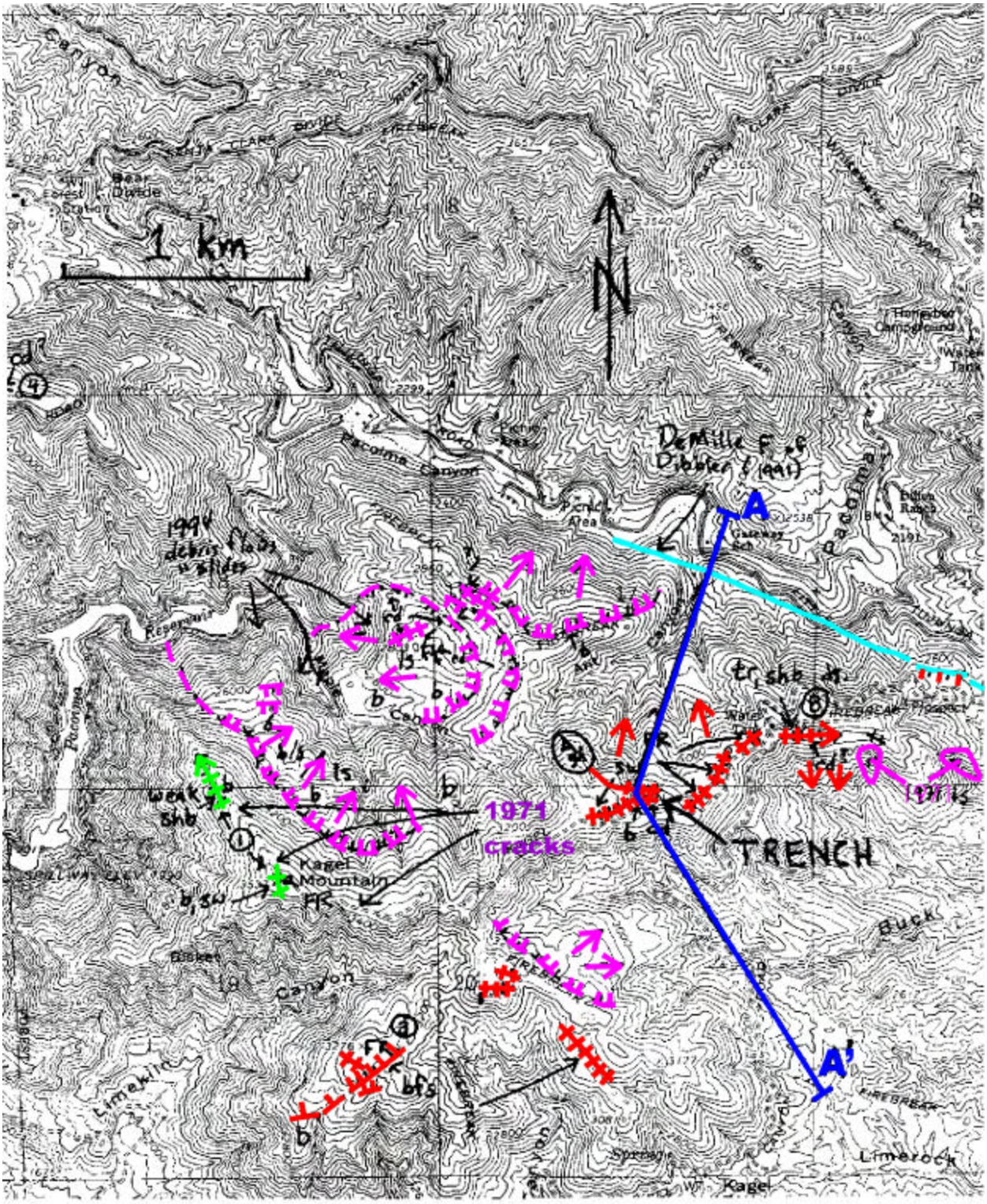

Fig. 14. Location map of the Kagel Mountain trench site, Sunland and San Fernando 7.5' quadrangles. See Fig. 2 for an explanation of symbols.

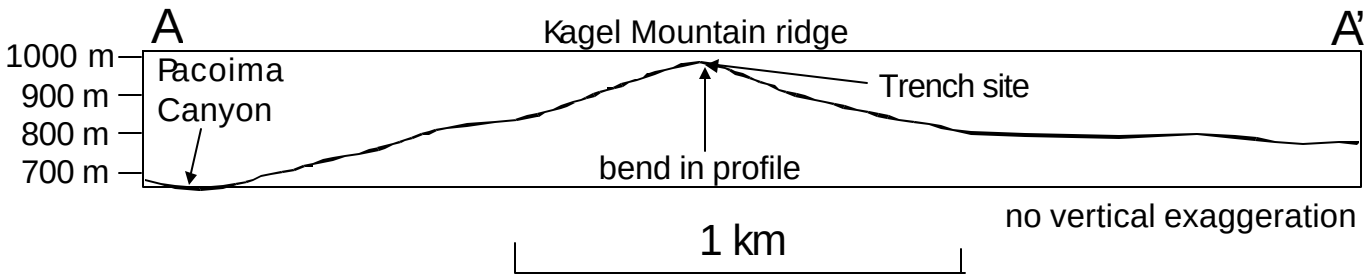

Fig. 15. Topographic profile of the Kagel Mountain ridge.

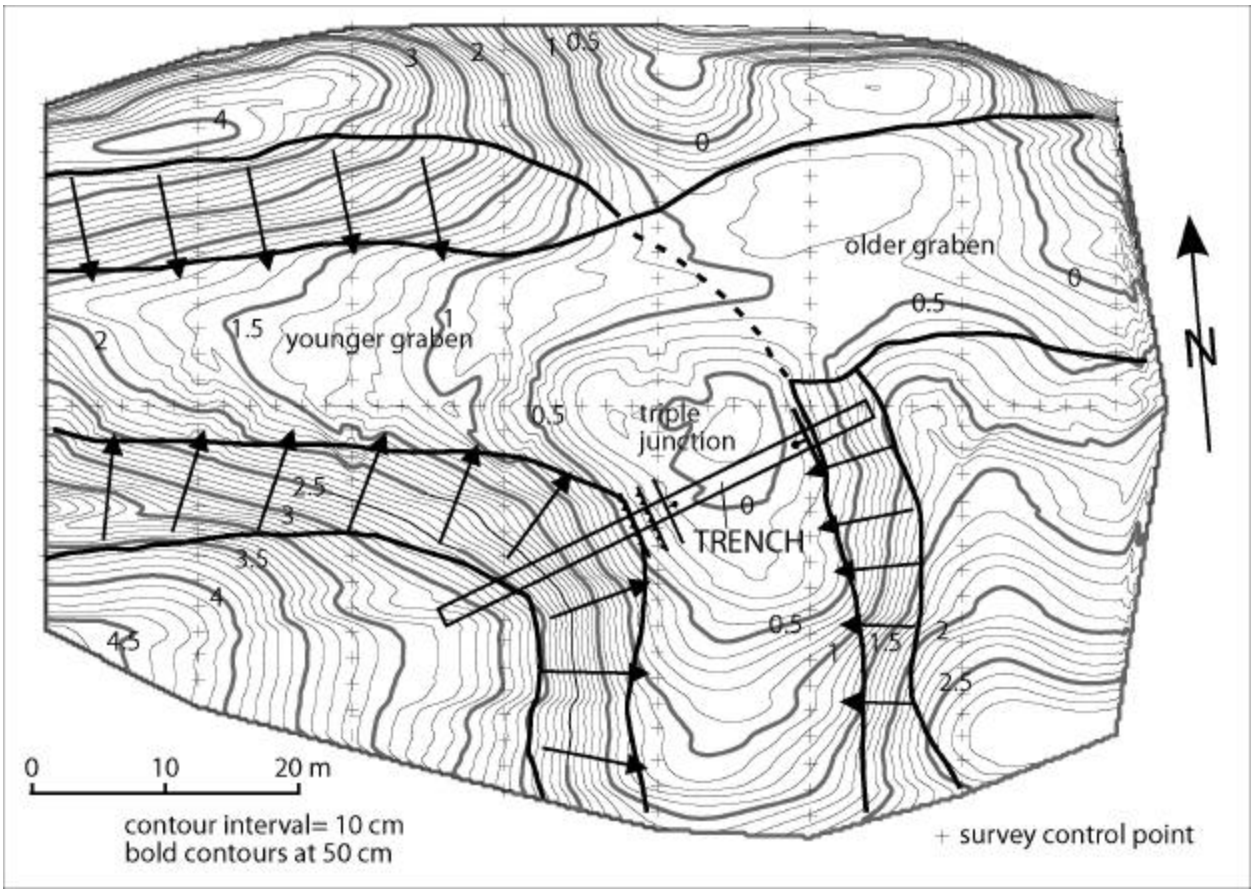

Fig. 16. Detailed topographic map of the Kagel Mountain trench site.

5.3 Structure

The closed depression we transected is the surface expression of a graben, defined by a narrower and simpler normal fault zone beneath the eastern scarp and a wider, more complex fault zone beneath the toe of the western scarp (Fig. 17). In both cases the faults underlay the toes of the topographic scarp. This geometry probably results from the upslope migration of the toe of the topographic scarp, caused by aggradational burial of the lower part of the scarp with locally-derived slopewash.

Unlike the other two trenches, this trench exposes a rather symmetrical graben with a flat bedrock floor, rather than a strongly tilted, asymmetrical half-graben. The better-developed normal "fault" zone (faults F1 and F2) underlies the lower part of the eastern scarp and is composed of two faults (Fig. 18). Fault F1 juxtaposes quartz diorite on the footwall against gneissic rocks on the hanging wall. The fault dips 60^{o} toward the trough axis and displaces the top of bedrock about 1.8 m vertically. The fault is composed of a 10-20 cm-thick shear zone in which granitic rock of the footwall has been shattered and rotated parallel to the fault plane. Some of this shear fabric may be inherited from episodes of faulting that predate the present topography. For example, given the change in rock type across this fault, its cumulative displacement is probably much greater than 1.8 m. Fault F2 is a smaller normal fault that displaces the top of bedrock (and its overlying residual soil) 35 cm vertically. It is actually composed of two parallel thin strands, but does not display a shear zone of any measurable width as does fault F1. Fault F2 probably extends upwards into unit 3, as indicated by the strong drag of that unit as it approaches fault F1.

Faults F3-F7 underlie the toe of the western scarp and exhibit a variety of styles and displacement amounts. Faults F3 and F4 are normal faults that dip toward the trough axis, whereas faults F5-F7 are reverse faults that parallel foliation in the gneissic rocks. Faults F3 and F4 have contributed to the structural development of the graben, because they: 1) cut across foliation as true graben faults, 2) they are associated with the margins of graben-filling deposits, and 3) they have displacements measured in 10s of cm. In contrast, faults F5-F7 do not cut across the gneissic foliation and have throws of only 10-15 cm. These faults probably accommodate flexural warping of the gneiss under the western scarp by slip on foliation planes. The same phenomenon also occurs on a even smaller scale on the three shear zones mapped between F7 and the western end of the trench; none of these "shear zones" displace the top of bedrock.

The western half of the trench contains numerous narrow (10-30 cm wide) zones of fractured or shattered rock that parallel the gneissic foliation, the larger of which are shown on Fig. 17. Many of these zones contain open joints and appear to have accommodated some NE-SW extension. As shown in Fig. 19, foliation strikes N05E and dips 60^{o}W. The widest joints (Joint 1), either open or filled, parallel this foliation. The second widest joints (Joint 2) strike roughly perpendicular to foliation and dip 52^{o}N. Joint sets 1 and 2 form a conjugate set that is essentially bisected by the local extension direction here (N65E). It appears that diffuse extension of bedrock in the western half of the trench has been accomplished, not by the formation of normal faults that strike parallel to the surface scarps and cut across bedrock foliation, but by the opening of joint sets 1 and 2. This same phenomenon was observed by McCalpin (unpub.) in 14 trenches on the Pajarito fault zone, New Mexico, where extension made use of pre-existing vertical cooling joints in the Bandelier (welded) tuff.

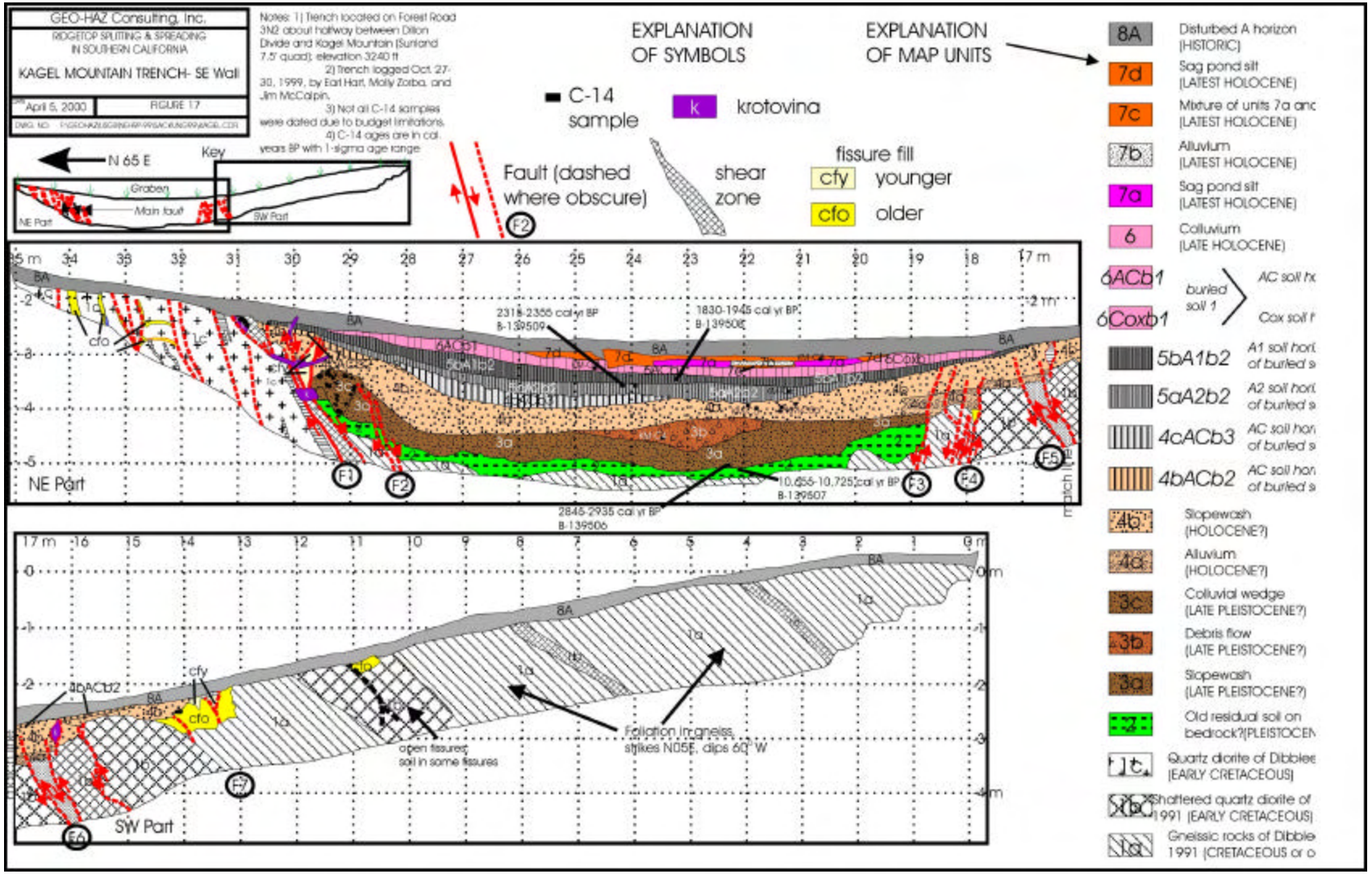

Fig. 17. Log of the Kagel Mountain trench.

Fig. 18. Photograph of faults F1 and F2 in the Kagel Mountain trench (red flags in wall in front of J.P. McCalpin, near ladder). Fault F1 juxtaposes fairly intact, foliated granite (light tones at far end of trench) against light brown scarp-derived colluvium (left center) and dark brown soil A horizons developed on sandy slopewash (center and right). Note the upward drag of the colluvium (units 3 and 4) as they approach the fault.

5.4 Stratigraphy

We defined two bedrock map units and 20 unconsolidated map units in this trench. All the unconsolidated units are contained in a single structural domain, i.e. the graben.

5.4.1 Bedrock Units

The NE end of trench is underlain by unit 1 c, which we correlate with the quartz diorite of Dibblee (1991). This rock exists only in the footwall of fault F1. It is composed of coarsely to very coarsely crystalline pinkish-gray granodiorite with quartz, feldspars (including pink orthoclase), and biotite (5-10%); slightly foliated and sheared parallel to foliation; contains leaves or dikes of leucocgranite (locally hard and fresh) and finely crystalline diorite (?) that is soft and very decomposed. Granodiorite is jointed and sheared with dominant shears striking N60W and dipping 70-80 degrees S. This strike roughly parallels the scarp at the NE end of the trench, but is different than the regional foliation mapped by Dibblee (1991) on this ridge (N35W, vertical). Rock is also moderately to highly decomposed; decomposition increases to SW in trench, being pronounced at the contact with graben-fill colluvium.

The western half of the trench is underlain by unit 1a, which we correlate with the older gneissic rocks of Dibblee (1991). Unit 1a is a well foliated gneiss with quartz, feldspar, and biotite (10-20%); finely to coarsely crystalline; moderately to highly decomposed; gray to brown colors (weathered); dip of foliation is moderate, but variable, to the SW; contains dikes and interleaves of leucocratic, coarse-grained granitic rock with very little biotite (unit 1b).

The trough is underlain by highly decomposed bedrock that resembles unit 1a more than 1b. Its advanced state of decomposition probably results from water infiltration through the overlying trough sediments.

5.4.2 Unconsolidated Units

Of the 20 unconsolidated map units we defined, 14 are parent materials unaffected by soil formation and 6 are soil horizons. The oldest parent material (unit 2) is a clast-poor clayey sand that directly overlies extremely weathered bedrock. The lower part of this unit is transitional with bedrock, and we interpret it as a residual soil. Its upper contact is also gradational upwards into unit 3a, a less clayey, massive, nonstratified silty sand with rare clasts. The lack of stratification and clasts suggests that unit 3a is a distal slopewash deposit derived from local areas. Between faults F1 and F2 unit 3 suddenly becomes very stony (unit 3c). From its location, shape, and texture we interpret unit 3c as a colluvial wedge shed from a free face of fault F1. In the center of the graben the uppermost part of unit 3 contains a lens-shaped area containing large angular clasts surrounded by sandy matrix (unit 3b). This deposit look like a small debris flow.

Above unit 3 is a less dense, softer, massive silty sand defined as unit 4b. Generally this unit resembles unit 3 in its lack of stratification and it is also interpreted as slopewash. Between faults F3 and F5 the lower part of unit 4b contains some moderately-sorted, weakly stratified lenses of gravel. We define this part as unit 4a. The upper part of unit 4 (unit 4c) has been overprinted by the lower part of a soil (an AC horizon). This soil comprises the third buried soil below the surface, so it is designated as 4cACb3, with 4c indicating the parent material, AC the horizon characteristics, and b3 the third buried soil from the surface. Importantly, units 2, 3, 4, and the 4cACb3 soil have all been dragged up to a dip of about 35^{o} by faults F1 and F2; this drag does not affect younger parent material or soils.

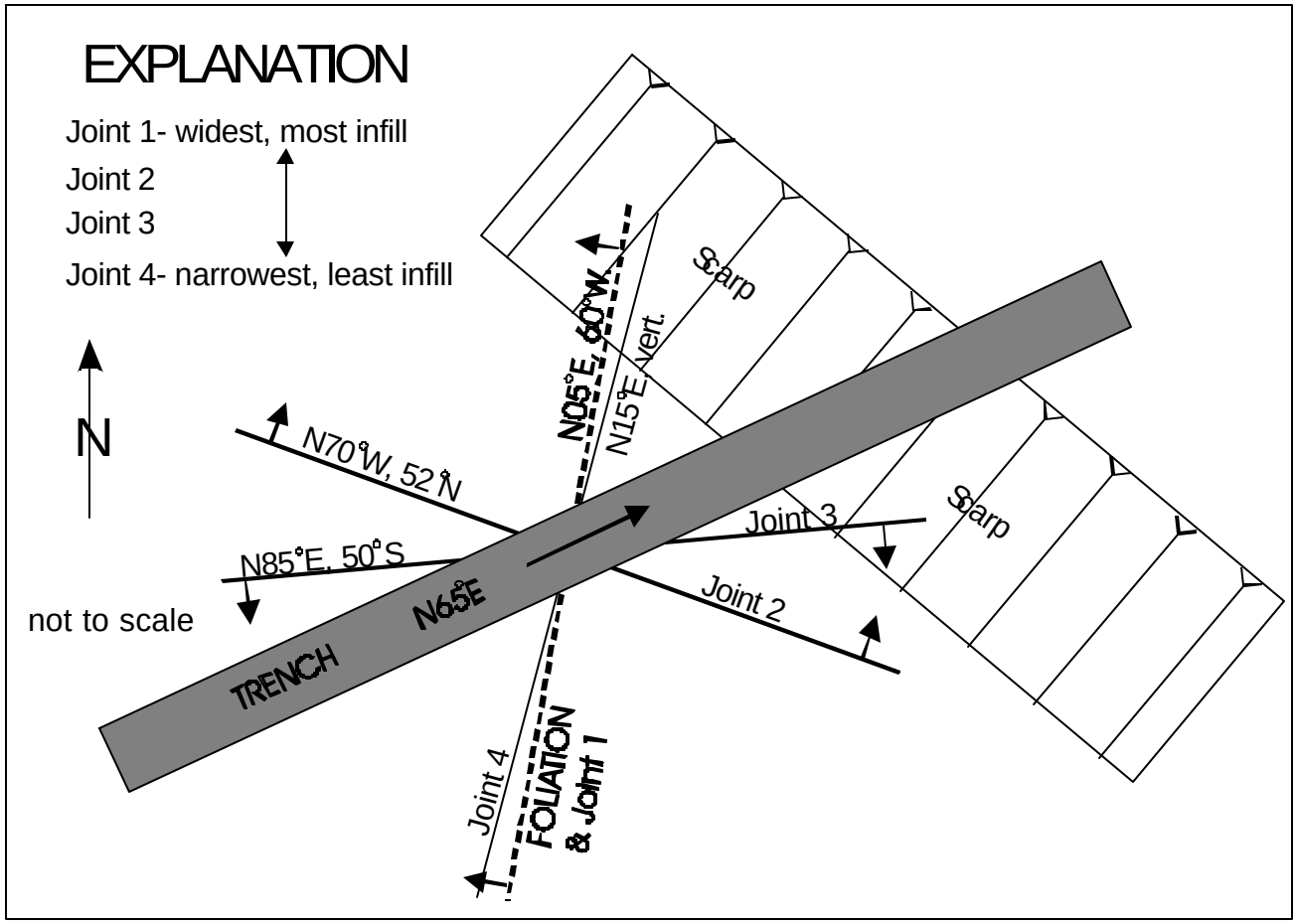

Fig. 19. Schematic diagram of joint and foliation directions in the Kagel Mountain trench.

The next youngest unit is unit 5, a clast-poor silty sand that defines a thin lens that tapers slowly to points beneath the toes of the scarps flanking the trough. Due to its thin nature, all of unit 5 is affected by soil formation, its two component horizons being 5aA2b2 and 5bA1b2. This soil is the second buried soil beneath the ground surface. Near faults F1 and F2 these units lap over the upturned, eroded edges of older parent materials and soils in angular unconformity.

Units 6 and 7 are very young (latest Holocene?) colluvium and sag pond deposits. Unit 6 contains a weak Ac/Cox soil profile (units 6ACb1 and 6CoxB1) and is more poorly sorted and more poorly stratified than unit 7. Unit 7 contains four members, two of which are finely laminated silts containing many mm-scale fining-upward cycles and abundant detrital charcoal and carbonized plant remains. These laminated silts suggest deposition in standing water and true sag pond conditions. Finally, the ground surface is underlain by unit 8A which forms the A horizon of the modern soil. This parent material appears to be an artificial mixture of silt through gravel, probably plowed up by bulldozers during construction of the ridgetop firebreak.

5.5 Geochronology

Eight radiocarbon samples were collected from the trench but only four could be dated due to budget constraints. The four C-14 ages are in correct stratigraphic order, but do not define a linear increase of age with depth. The two upper samples yield ages of 1830-1945 cal yr. BP (unit 5bA1b2) and 2315-2355 cal yr, BP (unit 5aA2b2) and define deposition rates of 0.37 m/ka and 0.40 m/ka, respectively. These rates are only slightly higher than the rates obtained at the Upper Lytle Creek Ridge trench (0.30-0.35 m/ka).

In contrast, the lower pair of samples yield anomalous ages. The base of unit 3a dates at 2845-2935 cal yr. BP, a mere 500-1000 years older than the upper pair of dates, but from a depth of 2.25 m below the ground surface. The sample from unit 2, collected only 10 cm lower (depth of 2.35 m) yields an age of 10,655-10,725 cal yr. BP. If these ages are correct it implies that: 1) the 1.3 m of sediment comprising units 3-5 was deposited in only 500 years, and 2) there is a major unconformity between units 2 and 3. The latter situation is possible, because unit 2 is interpreted as the soil developed on the pre-graben landscape. This soil may have developed over a long period of time and was then buried after the graben formed and graben-fill sediments began to accumulate. Coincidentally, an age of 10,655-10,725 cal yr. BP for the initial formation of the graben is similar to the extrapolated age of 8.5-10 ka for the initial formation of the graben at the Upper Lytle Creek Ridge trench.

However, if the graben initially formed at ca. 10.6-10.7 ka, why does the base of unit 3a date at 2.8-2.9 ka? This part of the stratigraphic section would have to represent the earliest graben-fill sediments, and they should date at ca. 10.5 ka. If we accept the upper two C-14 dates as accurate, then 1.3 m of sediment (units 3-5) plus two soils (b2 and b3) would have to form between ca. 2.9 ka (date from Unit 3) and 2.3 ka (date from unit 5aA2b2). This seems unreasonable. Units 3 and 4 are denser and more compact than the deposit 2ACb2 dated in the Upper Lytle Creek Ridge trench, which suggests an age greater than 4 ka, rather than 2.9 ka.

Alternative #1 is that the carbon dated from the base of unit 3a is intrusive and much younger than its host deposit. Granted, the sample was a very small fragment of charcoal, but so was the sample from unit 2. Alternative #2 is that the 10.6-10.7 ka date from unit 2 is erroneously old, which would require that the dated charcoal be a detrital piece that was 8000 years older than its host sediment. We are skeptical that charcoal could survive 8000 years in the near-surface environment before being

recycled into a younger deposit. Our preference at this time is to accept Alternative 1, because: 1) the remaining 3 dates define a more uniform deposition rate comparable to the other two trench sites, 2) the early Holocene age for graben initiation conforms with other sites and the degree of compaction and soil formation in the trough fill, and 3) it is unlikely that Alternative #2 is true.

5.6 Interpretation

Based on cross-cutting relationships and angular unconformities, two major episodes of displacement created this trough (Fig. 20). The earliest episode (Fault Event Y) formed the graben into which the major fill units (units 3 and 4) were deposited. In our reconstruction this event occurred after the formation of the residual soil on bedrock, after which this soil was conveniently eroded off the two footwalls. If we accept the C-14 age from unit 2, this event occurred shortly after 10,655-10,725 cal yr. BP. An alternative hypothesis is that the "residual soil" exposed the bottom of the trench wall is a water-related weathering phenomenon that only formed under the trough after it was formed, as a result of constant infiltration. we do not favor this alternative because we would expect to see some evidence of water ponding, gleying, and reduced soil colors (greens), and these are not present.

The existence of a colluvial wedge (unit 3c) abutting fault F1 suggests that the major displacement during this episode was on that fault, with smaller displacements on the faults F3-F5. If we assume the free face created during this event was roughly twice as high as the colluvium thickness (0.6 m), then the approximate vertical displacement on F1 in this event was 1.2 m.

Deposition of units 3 and 4 is inferred to have nearly filled the graben and buried the flanking scarps. This inference is supported by the burial of the gravelly colluvial wedge (unit 3c) by finer slopewash (unit 4). Such a fining upward sequence could probably not have occurred adjacent to the trough boundary if there was still a steep scarp on the surface.

Fault Event Z reactivated fault F1 and created fault F2, and resulted in warping units 3 and 4 from their original low dips to nearly 35^{o} near the faults. Minor movement on faults F3-F5 also occurred at this time. Vertical displacement across fault F2 is 35 cm, measured on the top of unit 2. The cumulative vertical displacement across fault F1, measured on the top of bedrock, is 2.5 m and represents both events Y and Z. If our earlier estimate of 1.2 m displacement for event Y is correct, then event Z caused about 1.3 m of vertical displacement on fault F1.

Following this event erosion beveled off the upturned edge of unit 4 and partly to completely removed its soil (4cACb3), after which unit 5 was deposited in the graben. The soil that subsequently formed in unit 5 is generally restricted to unit 5 (i.e., 5aA2B2 in its lower part, 5bAb2 in its upper part) in the center of the graben, but where unit 4 was truncated and unit 5 thins between faults F1 and F2, buried soil 2 is superimposed down into unit 4 (unit 4bACb3). Subsequently units 6, 7, and 8 were formed. There is no evidence of deformation of units younger than unit 4.

The above scenario assumes that Event Z occurred after the formation of horizon 4bACb3 (dated at 2315-2355 cal yr. BP) but before the formation of horizon 5bA1b2 (dated at 1830-1945 cal yr. BP). These two dates thus bracket Event Z as occurring between 1830 and 2355 cal yr. BP.

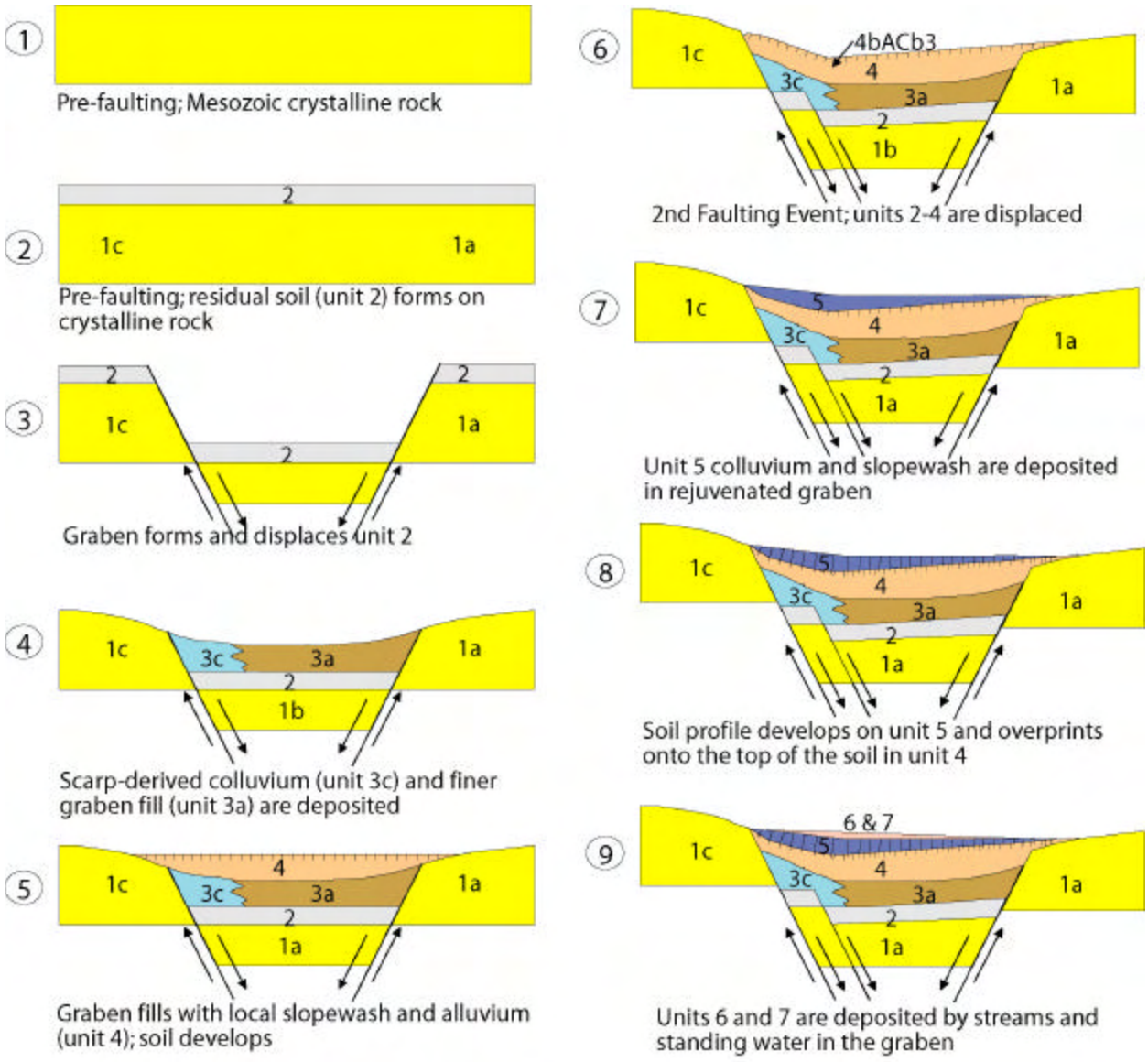

Fig. 20. Inferred sequence of events that formed the Kagel Mountain sackung.

The closest Holocene fault to the trench is the San Gabriel- De Mille system, traces of which lie at the foot of the ridge only 1.4 km and 1 km, respectively, from the trench site. According to Cotton et al. (1988), the latest surface-rupturing earthquake on the San Gabriel fault at Saugus (24 km NW of our trench) occurred between 907-1278 cal yr. BP and 1021-1992 cal yr. BP. This rather broad time range barely overlaps with the time window for event Z in the Kagel Mountain trench (Fig. 21). Cotton et al. (1988) did not measure the displacement during this event, but did document 4.5-6.6 m of cumulative displacement of Holocene (ca. 10-11 ka) deposits. Their trench logs indicate that deposits ca. 3.5 ka had only been faulted once. Therefore, the 4.5-6.6 m of right-lateral offset may represent only one or two paleoearthquakes. If one earthquake, then single-event displacements of 4.5-6.6 m imply earthquakes of M 7.6-7.7; if two earthquakes of similar size, single-event displacements of 2.2-3.3 m imply paleoearthquakes of M 7.4-7.5. The lateral extent of the MRE on the San Gabriel fault is not known.

6. DISCUSSION--ORIGIN ON RIDGETOP SPREADING IN SOUTHERN CALIFORNIA

Two of the three trenched ridgecrest troughs were the surface expressions of half-grabens with moderately dipping (45^{o}-65^{o}) normal faults, whereas the third trough was underlain by a more symmetrical graben. The higher and steeper scarp on the surface did not necessarily overlie the master fault. In fact, at all three sites the higher surface scarp was developed on the hinged side of the graben, whereas the scarp atop the master fault was smaller but steeper. The 1-3 m of unconsolidated Holocene (?) slopewash beneath each trough was relatively coarse-grained (sand and gravelly sand) and poorly stratified. Accordingly, the main contacts mapped in these deposits were soil horizon boundaries. In places it was difficult to distinguish whether changes in color and texture were parent material contacts or soil horizon contacts.

The lower boundary of slopewash was gradational with weathered bedrock. The bedrock beneath the troughs was either extensively shattered (which we defined as "exploded bedrock") or chemically weathered from infiltration of water beneath the closed depression, much more so than beneath the flanking scarps.

Each trench exhibited stratigraphic evidence for 2-4 discrete displacement events, but not all events could be tightly dated (Fig. 21). In the Blue Ridge and Upper Lytle Creek Ridge trenches, the latest deformation event occurred after 790-867 cal yr. BP but before 285-300 cal yr. BP. This time span overlaps the age ranges of three dated paleoearthquakes on the San Andreas fault at the Wrightwood paleoseismic site of Fumal et al. (1993), only a few km northwest of the Blue Ridge trench. The relatively small number of radiocarbon samples that we dated from each trench was not sufficient to make a positive correlation with any particular paleoearthquake on the San Andreas fault.

The older displacement events at Blue Ridge and Upper Lytle Creek Ridge are generally older than the oldest dated event in the Wrightwood or Pallet Creek chronologies. At the Blue Ridge trench, events older than the MRE cannot be well constrained by the available C-14 dates. For example, the penultimate event occurred sometime before 1055-1165 cal. yr BP, but it could have occurred several hundred to thousand years before those dates. A crude estimate of recurrence times for deformation events at Blue Ridge can be calculated from the occurrence of four events since the beginning of the Holocene (ca. 10 ka), the latest of which occurred at ca. 300-700 cal yr BP. If the previous ca. 9.5 ka contained three events uniformly spaced in time (four intervals), then a long-term mean recurrence of 2.4 ka is indicated. This mean recurrence is much longer than the 150-300 year recurrence of M8 earthquakes on the San Andreas fault

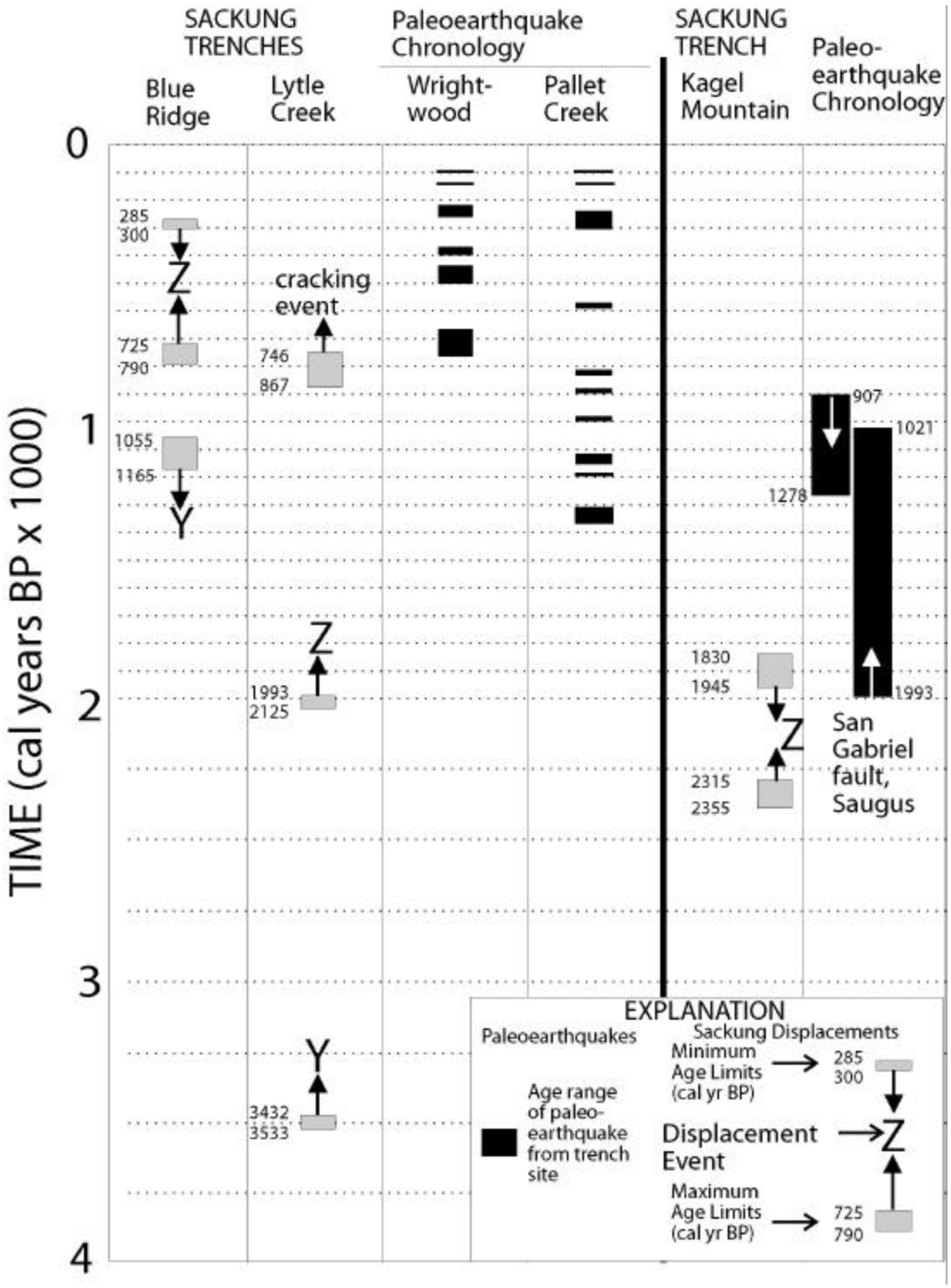

Fig. 21. Space-time diagram showing ages of displacement events in our sackung trenches, versus ages of dated paleoearthquakes on nearby major active faults. The nearest fault to the Blue Ridge and Upper Lytle Creek Ridge trenches is the San Andreas fault, which was studied at Wrightwood (Biasi and Weldon, 1998), and at Pallett Creek (Sieh et al, 1989). The nearest fault to the Kagel Mountain trench is the San Gabriel-De Mille fault system (Cotton et al, 1988).

yr. BP. This time span overlaps the age ranges of three dated paleoearthquakes on the San Andreas fault at the Wrightwood paleoseismic site of Fumal et al. (1993), only a few km northwest of the Blue Ridge trench. The relatively small number of radiocarbon samples that we dated from each trench was not sufficient to make a positive correlation with any particular paleoearthquake on the San Andreas fault.

The older displacement events at Blue Ridge and Upper Lytle Creek Ridge are generally older than the oldest dated event in the Wrightwood or Pallet Creek chronologies. At the Blue Ridge trench, events older than the MRE cannot be well constrained by the available C-14 dates. For example, the penultimate event occurred sometime before 1055-1165 cal. yr BP, but it could have occurred several hundred to thousand years before those dates. A crude estimate of recurrence times for deformation events at Blue Ridge can be calculated from the occurrence of four events since the beginning of the Holocene (ca. 10 ka), the latest of which occurred at ca. 300-700 cal yr BP. If the previous ca. 9.5 ka contained three events uniformly spaced in time (four intervals), then a long-term mean recurrence of 2.4 ka is indicated. This mean recurrence is much longer than the 150-300 year recurrence of M8 earthquakes on the San Andreas fault.

At the Upper Lytle Creek Ridge trench the two latest displacement events (Events Y and Z in Fig. 13) occurred just after 3432-3533 cal yr BP and just after 1993-2125 cal yr BP, respectively, a time span of 1307-1540 years. This value is similar to the mean recurrence one would calculate knowing only that there had been two events after 3533 cal yr BP (three intervals in 3533 years= 1178 years). In contrast, Events W and X occurred in the time period between 8.5-10 ka and 3.5 ka, a time span of 5-6.5 ka. With only two interevent times in this time span, a mean recurrence of 2.5-3.2 ka is indicated, or roughly twice as long as the period between dated Events Y and Z. This apparent variation may reflect a true variation in recurrence, or may reflect the fact that additional deformation events occurred between our Events W and Y that we could not identify in the trench.

The latest displacement event at the Kagel Mountain site is relatively well bracketed between 1830 and 2355 cal yr. BP. This age range barely overlaps with the age range of the latest paleoearthquake on the San Gabriel fault, the closest active fault to the site, as dated by Cotton et al between 907 and 1993 cal. yr BP. Alternatively, the MRE at this site could coincide with the MRE on a segment of the Sierra Madre fault which probably underlies the ridge. Lindvall et al. (1999) estimate the MRE on the western part of the Sierra Madre fault in the Glendale area occurred about 7 ka. Due to the ambiguity of dating the earlier event, we cannot calculate a meaningful recurrence interval.

7. CONCLUSIONS

1) Trenching at each of the three sites demonstrates that repeated ground rupture occurs along ridgetop depressions. That these anomalous ridgetop depressions are formed by ground rupture during large earthquakes has been demonstrated after the 1989 Loma Prieta earthquake (Hart et al., 1990; Spittler and Harp, 1990; Ponti and Wells, 1991) and other earthquakes. That earthquakes caused the anomalous ridgetop depressions has not been conclusively demonstrated by our study, but all of the most recent events at each of the trench sites are consistent with known paleoearthquakes on nearby active faults.

2) Our trenching clearly demonstrates that repeated ruptures coincided with existing scarps that define ridgetop depressions, As much as a meter or more of vertical displacement can occur during these rupture events. The observed ruptures penetrate bedrock and are similar to tectonic rupture along

normal faults. Because these rupture events are equivalent in frequency (2-4 events in ca. 10,000 years) and magnitude to ruptures on normal faults in California, ridgetop depressions and scarps pose a hazard to structures that may be sited on ridgetops and should be evaluated and avoided as if they were tectonic faults. CDMG may wish to consider zoning these features, perhaps as part of its Seismic Hazards Zoning program since these fault-like features appear to be incipient landslide features.

3) Based on our previous study (McCalpin and Hart, 1999), the anomalous ridgetop depressions appear to form a continuum with landslides and to have the same causal mechanisms.

4) Not all deformation events may have been recognized, especially smaller events that mainly produced fissuring.

8. RECOMMENDATIONS

Although we have demonstrated that sackung troughs contain a stratigraphic record of repeated displacement events that can be dated, we fell short of our goal of making a one-to-one match of sackung displacement events with dated paleoearthquakes. In hindsight, it was naive for us to think that we could compare our sackung chronologies, based on one limiting C-14 date per event, with paleoearthquake chronologies supported by many C-14 dates per event. We recommend that additional trenching studies of ridgetop depressions, supported by larger dating budgets more like those of fault trenching studies, would decrease the uncertainty in dating sackung events, and make a better event-to-paleoearthquake correlation possible. As a guess, it will probably require 2-3 times as many radiocarbon dates as we had budgeted for to bracket event dates well enough to compare them with paleoearthquake chronologies from trench studies.

9. REFERENCES

Barrows, A.G., Irvine, P.J., and Siang, S.T., 1995, Geologic surface effects triggered by the Northridge earthquake in M.C. Woods and W.R. Seiple, editors, The Northridge, California, Earthquake of 17 January 1994: California Division of Mines and Geology Special Publication 116, p. 65-88.

Barrows, A.G., Kahle, J.E., Weber, F.H., Jr., Saul, R.B., and Morton, D.M., 1974, Surface effects maps of the San Fernando earthquake area: California Division of Mines and Geology Bulletin 196, pl. 3.

Biasi, G. and Weldon, R.J., 1998, Paleoseismic date refinement and implications for seismic hazard estimation, in Sowers, J.M. et al. (eds.), Dating and earthquakes; Review of Quaternary geochronology and its application to paleoseismology: Wm. Lettis & Assoc., Walnut Creek, CA, US Nuclear Regulatory Commission, NUREG 5562, p. 3-61 to 3-66.

Birkeland, P.W., 1999, Soils and geomorphology: Oxford University Press, NY, 432 p.

Bonilla, M.G. and Lienkaemper, J.J., 1991, Factors affecting the recognition of faults exposed in exploratory trenches: U.S. Geological Survey Bulletin 1947, 54 p., 1 microfiche.

Cotton, W.T., Fowler, W.L. and Hay, E.A., 1988, Late Pleistocene and Holocene paleoseismicity of the San Gabriel fault, Saugus/Castaic area, Los Angeles County, California: unpub. Final Technical Report submitted by Wm. Cotton & Associates, Los Gatos, CA to the U.S. Geological Survey, contract no. 14-08-0001-G1196, 21 p. plus 6 oversize plates.

Dibblee, T.W. Jr., 1991, Geologic map of the Sunland and Burbank (North 1/2) quadrangles, Los Angeles County, California: Dibblee Geological Foundation, Map #DF-32, scale 1:24,000.

Dolan, J.F., Sieh, K., Rockwell, T.K., Guptill, P. and Miller, G., 1997, Active tectonics, paleoseismology, and seismic hazards of the Hollywood fault, northern Los Angeles Basin, California: Geol. Soc. Amer. Bull, 109(12): 1595-1616.

Fumal, T.E., Pezzopane, S.K., Weldon, R.J. II, and Schwartz, D.P., 1993, A 100-year average recurrence interval for the San Andreas fault at Wrightwood, California: *Science*, **259**, 199-203.

Harp, E.L., and Jibson, R.W., 1996, Landslides triggered by the 1994 Northridge Calfornia earthquake: Bulletin of the Seismological Society of America, v. 86, n. 1B, p. S319-S332, pl. 1.

Hart, E.W., Bryant, W.A., Wills, C.J., and Treiman, J.A., 1990, The search for fault rupture and significance of ridgetop fissures, Santa Cruz Mountains, California in S.R. McNutt and R.H. Sydnor, editors, The Loma Prieta earthquake of 17 October 1989: California Division of Mines and Geology Special Publication 104, p. 83-94.

Hartzell, S.H., Carver, D.L., and King , K.W., 1994, Initial investigation of site and topographic effects at Robinwood Ridge, California: Bulletin of the Seismological Society of America, v. 84, p. 1336-1349

Jennings, C. W., and Strand, R. G., 1969, Geologic Map of California Los Angeles sheet: California Division of Mines and Geology, Olaf P. Jenkins Edition.

Lindvall, S.C., Rockwell, T.K., Walls, C. and Rubin, C.M., 1999, Large-slip earthquakes and uplift rate gradient on the Sierra Madre-Cucamonga fault zone, southern Transverse ranges: Geol. Soc. Amer. Abs. With Programs 31(6):75.

McCalpin, J.P., 1996a, Paleoseismology of Extensional Tectonic Environments, Chapter 3 in McCalpin, J.P. (ed.), Paleoseismology: Academic Press, New York, p.85-146

McCalpin, J.P., 1996b, Field Techniques in Paleoseismology, Chapter 2 in McCalpin, J.P. (ed.), Paleoseismology: Academic Press, New York, p.33-84.

McCalpin, J.P. and Hart, E.W.., 1999, Ridgetop splitting, spreading, and shattering related to earthquakes in southern California: unpublished Final Technical Report submitted to U.S. Geological Survey by GEO-HAZ Consulting, Inc., Contract 1434-HQ-GR-1026, April 23, 1999, 44 p. plus appendices, 4 plates.

McCalpin, J.P. and Nelson, A.R., 1996, Introduction to Paleoseismology, Chapter 1 in McCalpin, J.P. (ed.), Paleoseismology: Academic Press, New York, p.1-32.

McCrink, T.P., 1995, Ridge-top landslide triggered by the Northridge earthquake: California Division of Mines and Geology Special Publication 116, p. 273-278.

Miller, W.J., 1934, Geology of the western San Gabriel Mountains of California: Univ. of California Publications in Mathematics and Physical Sciences, v. 1, no. 1, p. 1-114.

Morton, D.M. and Sadler, P.M., 1989, The failings of the Pelona Schist; landslides and sackungen in the Lone Pine Canyon and Wrightwood areas of the eastern San Gabriel Mountains, southern California, in Sadler, P.M. and Morton, D.M. (eds.), Landslides in a semi-arid environment, with emphasis on the inland valleys of southern California: Inland Geological Society, Publication 2, p. 301-322.

Morton, D.M., Woodburne, M.D., and Foster, J.H., 1991, Geologic map of the Telegraph Peak quadrangle, San Bernardino County, California: U.S. Geological Survey Open-File Report 90-693, 10 p., 2 pl.

Nolan, J.M. and Webber, G.E., 1992, Evaluation of surface cracking caused by the 1989 Loma Prieta earthquake, Santa Cruz County, California: Case histories, in Sharma, S. (ed.), Proceedings of the 28th Symposium on Engineering Geology and Geotechnical Engineering: University of Idaho, Moscow, ID, p. 272-286.

Ponti, D.J., and Wells, R.E., 1991, Off-fault ground ruptures in the Santa Cruz Mountains, California: Ridge-top spreading versus tectonic extension during the 1989 Loma Prieta earthquake: Bulletin of the Seismological Society of America, v. 81, p. 1480-1510.

Radbruch-Hall, D.H., Varnes, D.J., and Savage, W.Z., 1976, Gravitational spreading of steep-sided ridges ("sackung") in western United States: International Association for Engineering Geology Bulletin, v. 14, p. 23-35.

Radbruch-Hall, D.H., Varnes, D.J., and Colton, R.B., 1977, Gravitational spreading of steep-sided ridges in Colorado: U.S. Geological Survey Journal of Research, v. 5, p. 359-363.

Radbruch-Hall, D.H., 1978, Gravitational creep of rock masses on slopes, in Voight, B. (ed.), Rockslides and avalanches, v. 1, p. 607-657: Elsevier, Amsterdam.

Rosenberg, L.I., 1990, Geological evaluation and soil engineering study, existing damage DeBoi residence, north Monterey County, California: Applied Soil Mechanics, unpublished consulting report prepared for American Red Cross, 39 p., 3 apps. (incomplete report filed with CDMG as C-921).

Sieh, K.E., Stuiver, M., and Brillinger, D., 1989, A more precise chronology of earthquakes produced by the San Andreas fault in southern California: Journal of Geophysical Research, v. 94, P. 603-623.

Spittler, T.E., and Harp, E.L., 1990, Preliminary map of landslide features and coseismic fissures triggered by the Loma Prieta, California, earthquake of October 17, 1989: California Division of Mines and Geology, Open-File Report 90-06, scale 1:4,800. (Same as USGS OF 90-688.)

Tabor, R.W., 1971, Origin of ridge-top depressions by large-scale creep in the Olympic Mountains, Washington: Geological Society of America Bulletin, v. 82, p. 1811-1822.

Technical Advisory Group on the Santa Cruz Geologic Hazard Investigation, 1991, Geologic hazards in the Summit Ridge area of the Santa Cruz Mountains, Santa Cruz County, California, evaluated in response to the 17 October 1989 Loma Prieta earthquake: Report of Technical Advisory Group: U.S. Geological Survey Open-File Report 91-618, 427 p., plates.

Varnes, D.J., Radbruch-Hall, D.H., and Savage, W.Z., 1989, Topographic and structural conditions in areas of gravitational spreading of ridges in the western United States: U.S. Geological Survey Professional Paper 1496, 28p.

Wells, R.E., Ponti, D.J., Clark, M.M., Bucknam, R.C., Budding, K.E., Fumal, T.E., Harwood, D.S.,Lajoie, K.R., Lienkaemper, J.J., Machette, M.N., Prentice, C.S., and Schwartz, D.P., 1989, Preliminary map of fractures formed in the Summit Road-Skyland Ridge area during the Loma Prieta, California, earthquake of October 17, 1989: U.S. Geological Survey Open-File Report 89-686, 1 plate, scale 1:12,000.

Zischinsky, U., 1966, On the deformation of high slopes: International Society of Rock Mechanics, 1st Congress, Proceedings, v. 2, p. 179-185.

Zischinsky, U., 1969, Uber sackungen: Rock Mechanics, v. 1, p. 30-52.